



RETURNING MATERIALS:

Place in book drop to
remove this checkout from
your record. FINES will
be charged if book is
returned after the date
stamped below.

--	--	--

HEAT CONDUCTION ACROSS A BENT PLATE
AND THE EFFECT OF CURVATURE ON THE
TEMPERATURE DISTRIBUTION

By

Abbas Arjomandi

A THESIS

Submitted to
Michigan State University
in partial fulfillment of the requirements
for the degree of

MASTER OF SCIENCE

Department of Mechanical Engineering

1985

ACKNOWLEDGEMENTS

The author wishes to express his thanks to his major professors, C.Y. Wang and Dr. Chuck Bartholomew, both faculty members of mechanical engineering, for their suggestions, guidance and encouragements throughout this study.

The author also wishes to thank professors James V. Beck and Dr. John J. Mcgrath for serving as members of his committee.

TABLE OF CONTENTS

LIST OF TABLES	v
LIST OF FIGURES	vii
NOMENCLATURE	ix
CHAPTER I Introduction	1
1.1 <u>Review of Literature</u>	1
1.2 <u>The Objective of This Study</u>	2
CHAPTER II Formulation of the Problem	5
2.1 <u>Coordinate System</u>	5
2.2 <u>Transformation to a Round Corner</u>	8
2.3 <u>Parameters</u>	9
CHAPTER III Finite Difference Method	13
3.1 <u>Boundary Conditions</u>	13
3.2 <u>Formulation for the Interior Nodes</u>	14
3.3 <u>Formulation for the Boundary Conditions</u>	18
3.4 <u>Node Generation</u>	20
3.5 <u>Computer Program</u>	21
3.6 <u>Temperature Distribution Along η-axis</u>	21
3.7 <u>Heat-transfer and Shape Factor</u>	25
3.8 <u>Isotherms</u>	28
3.9 <u>Error Estimate</u>	29
CHAPTER IV Results and Conclusions	31
4.1 <u>Numerical Results</u>	31

4.2 <u>Conclusion</u>	33
APPENDIX	80
LIST OF REFERENCES	85

LIST OF TABLES

Table 1:	Dimensionless temperatures along η -axis when $b = 2.0$	36
Table 2:	Dimensionless temperatures along s -axis when $b = 2.0$	37
Table 3:	Dimensionless temperatures along η -axis when $\theta = \pi/4$ and ε varies	38
Table 4:	Dimensionless temperatures along s -axis when $\theta = \pi/2$ and ε varies	39
Table 5:	Dimensionless temperatures along η -axis when $\theta = 3\pi/4$ and ε varies	40
Table 6:	Dimensionless temperatures along s -axis when $\theta = \pi$ and ε varies	41
Table 7:	Dimensionless temperatures along s -axis when $\theta = 3\pi/2$ and ε varies	42
Table 8:	Dimensionless temperatures along η -axis when $\theta = 2\pi$ and ε varies	43
Table 9:	Dimensionless temperatures along η -axis when $\theta = \pi/4$ and b varies	44
Table 10:	Dimensionless temperatures along η -axis when $\theta = \pi/2$ and b varies	45
Table 11:	Dimensionless temperatures along η -axis when $\theta = 3\pi/4$ and b varies	46
Table 12:	Dimensionless temperatures along η -axis when $\theta = \pi$ and b varies	47
Table 13:	Dimensionless temperatures along s -axis when $\theta = 3\pi/2$ and b varies	48
Table 14:	Dimensionless temperatures along s -axis when $\theta = \pi/4$	49

Table 15:	Dimensionless temperatures along s-axis when $\theta = \pi/2$	50
Table 16:	Dimensionless temperatures along s-axis when $\theta = 3\pi/4$	51
Table 17:	Dimensionless temperatures along s-axis when $\theta = \pi$	52
Table 18:	Dimensionless temperatures along s-axis when $\theta = 3\pi/2$	53
Table 19:	The dimensionless penetration depth along s-axis to reach the linear values for flat plate	54
Table 20:	The dimensionless temperatures at the indicated nodes when $\theta = \pi/4$	55
Table 21:	The dimensionless temperatures at the indicated nodes when $\theta = \pi/2$	56
Table 22:	The dimensionless temperatures at the indicated nodes when $\theta = 3\pi/4$	57
Table 23:	The dimensionless temperatures at the indicated nodes when $\theta = \pi$	58
Table 24:	The dimensionless temperatures at the indicated nodes when $\theta = 3\pi/2$	59
Table 25:	The shape factors and heat transfer ($q/K\Delta T_0$)	60
Table 26:	The dimensionless maximum temperature deficiencies and their locations along the η -axis	61
Table 27:	Dimensionless temperatures at two loca- tions along the η -axis when h varies and also at $s = b/2$ along the s-axis when l varies	62

LIST OF FIGURES

Figure 1:	"90 degree bend with straight boundaries"	4
Figure 2:	The Bent Plate and (η, s) Coordinate System	6
Figure 3:	Bent Plates With $b=4.0$ and (a) $\theta=\pi$, (b) $\theta=3\pi/2$, (c) $\theta=2\pi$, (d) $\theta=\pi/4$, (e) $\theta=\pi/2$ and (f) $\theta=3\pi/4$	10
Figure 4:	Bent Plates With $\theta=2\pi$ for a,b,c and d, $\theta=\pi/2$ for i,j,k and l $\theta=\pi/4$ for e,f,g and h	11
Figure 5:	Bent Plates When $\theta=\pi$ for a,b,c and d, $\theta=3\pi/2$ for e,f,g and h, $\theta=3\pi/4$ for i,j,k and l	12
Figure 6:	Representation of Boundaries and Boundary Conditions	15
Figure 7:	Representation of Nodes	22
Figure 8:	Computer Flowchart	23
Figure 9:	Showing the temperature deficiency along η -axis	26
Figure 10:	The isotherms when $\theta=\pi/2$ and $b=4.0$	30
Figure 11:	Dimensionless Temperatures along s-axis when $b=2.0$	63
Figure 12:	Dimensionless Temperatures along η -axis when $b=2.0$	64
Figure 13:	Dimensionless Temperatures along s-axis when $\theta=\pi/4$	65
Figure 14:	Dimensionless Temperatures along s-axis when $\theta=\pi/2$	66
Figure 15:	Dimensionless Temperatures along s-axis when $\theta=3\pi/4$	67

Figure 16:	Dimensionless Temperatures along s-axis when $\theta=\pi$	68
Figure 17:	Dimensionless Temperatures along s-axis when $\theta=3\pi/2$	69
Figure 18:	Dimensionless Temperatures along η -axis when $\theta=\pi/4$	70
Figure 19:	Dimensionless Temperatures along η -axis when $\theta=\pi/2$	71
Figure 20:	Dimensionless Temperatures along η -axis when $\theta=3\pi/4$	72
Figure 21:	Dimensionless Temperatures along η -axis when $\theta=\pi$	73
Figure 22:	Dimensionless Temperatures along η -axis when $\theta=3\pi/2$	74
Figure 23:	Dimensionless Temperatures along η -axis when $\theta=2\pi$	75
Figure 24:	Location of the intersection of the different isotherms with η -axis when $\theta=\pi/2$	76
Figure 25:	The Dimensionless Temperatures versus h at Two Locations Along η -axis	77
Figure 26:	The Dimensionless Temperatures versus h^2 at Two Locations Along the η -axis	78
Figure 27:	The Dimensionless Temperatures at $s=b/2$ Along the s-axis verses l (bottom line) and l^2 (top line)	79

NOMENCLATURE

Letters

a	Half of the plate thickness (m)
A	Matrix A
b	Half of the curve-length of the bend (dimensionless)
B	Matrix B
h_o	Convective heat transfer coefficient
h	The mesh length along η -axis (dimensionless)
k	Dimensionless curvature of the centerline
K	Conduction heat transfer coefficient
K'	Curvature of the centerline $[m]^{-1}$
l	Dimensionless number equal to $[l]^2/[h]^2$
R_c	Dimensionless radius of curvature of the centerline
R_i	Dimensionless radius of curvature of the interior boundary
R_o	Dimensionless radius of curvature of the exterior boundary
S	Dimensionless S coordinate along s-axis
S'	Dimensional S' coordinate along S'-axis [m]
T_o	Dimensional temperature of the interior surface $[C^\circ]$

x

T_l	Dimensional temperature of the exterior surface [C°]
T	Dimensional ambient temperature [C°]
$T_{m,n}$	Temperature at node (m,n) [C°]
$T_{i,j}$	Temperature at node (i,j) [C°]
ΔT_o	Overall temperature difference [C°]
x', x	x coordinate [m]
y', y	y coordinate [m]
z', z	z coordinate [m]

Greek Symbols

Δ	The difference between two quantities
θ	The central angle of the bend
χ	Dimensionless temperature
η'	η' -coordinate along η' -axis [m]
η	η -coordinate along η -axis [dimensionless]
α	The subdivision of θ where $\alpha = \theta/12$
ϵ	A small number equal to a/R_c
$\partial () / \partial ()$	Showing partial derivative

Vectors

\hat{N}	Unit vector along η' -axis
\hat{R}	Position vector for points along the center-line
\hat{i}	Unit vector along x-axis
\hat{j}	Unit vector along y-axis
\hat{k}	Unit vector along z-axis

ABSTRACT

HEAT CONDUCTION ACROSS A BENT PLATE AND THE EFFECT OF CURVATURE ON THE TEMPERATURE DISTRIBUTION

By

Abbas Arjomandi

Due to the complicated geometry, the heat conduction across a bent plate and the effect of curvature on the temperature distribution has never been studied before. The corner of a bent plate is a fundamental structural element which is susceptible to failure. By using the temperature distribution, the thermal-stress can be determined.

In this paper, an intrinsic coordination system is utilized in order to obtain a simpler form of the governing differential equation when compared with the cartesian coordinate formulation and then the equations are solved numerically. The results indicate the dependence of temperatures on the curvature and angle of the bend. The temperatures are decreased in the vicinity of the bend when compared to the linear distribution for flat plate having the same thickness.

A discussion on the influence of these parameters on the shape factor and rate of heat transfer is presented, and the accuracy of the results has a confidence level of three significant digits.

CHAPTER I

Introduction

1.1 Review of Literature

The steady-state heat conduction across a bent plate and the effect of curvature on the temperature distribution is the topic of this study. This information can be used in the design of pressure vessels or any situation where two different temperature fluids or gases are separated by a given plate geometry. Since the bend is most susceptible to failure, the results can also be used to determine the limiting thermal stresses. Carslaw [1] was the first to consider the effects of a bent element on heat transfer. He studied "a right angled bend in a wall" where both the interior and exterior angles of the bend were 90° , with no bends or curves involved. Figure 1 shows the details. Carslaw used the Schwarz-Christoffel transformation during the solution of the problem.

It was Ozisik [7] who was the first to solve the same problem using a finite difference method. Ozisik showed how to formulate the problem when all the boundaries were straight lines.

If the plate is flat or has the shape of a circular cylinder, exact solutions for the problem exist [3]. The present paper studies the case where the plate is neither completely straight nor circular. Separation of variables or conformal mappings are useless in this case. Furthermore, there has not been any analytical treatment of the problem until recently. C.Y. Wang [5] has recently applied an intrinsic coordinate system to the problem and solved it analytically for small perturbations.

He concluded that in the vicinity of the bend, the temperatures are decreased when compared to their corresponding linearly distributed values for a flat plate. The maximum decrease occurs at $S=0$, $\eta=0$ which corresponds to the center of the bend. Wang noticed that as the length of the bend ($2b$) is decreased, the temperatures tend toward the linear values of a flat plate.

The decrease of temperatures also vanished as $2b$ tended toward zero. He concluded that the local heat transfer changed as the curvature (or $2b$) changed, but to the order that problem was solved the total heat transfer is unchanged.

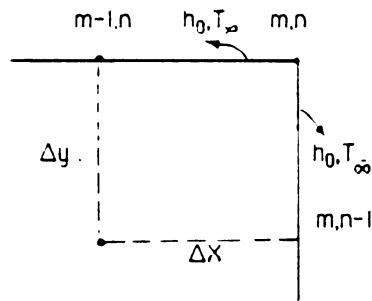
1.2 The Objective of this Study

The purpose of this study is to investigate the effect of curvature on the temperature distributions and heat transfer across a bent plate for steady-state heat conduction using the finite difference method. An

analytical method based upon a perturbation solution is possible if ratio of the plate width to local radius of curvature is very small. This restriction is not necessary for the finite difference method.

(a)-Exterior corner with convective boundary

$$2(h\Delta X/k)T_{\infty} + (T_{m-1,n} + T_{m,n-1}) - 2((h\Delta X/k) + 1)T_{m,n} = 0$$



(b)-Interior corner with convective boundary.

$$2(h\Delta X/k)T_{\infty} + 2T_{m-1,n} + 2T_{m,n+1} + T_{m+1,n} + T_{m,n-1} - 2(3 + h\Delta X/k)T_{m,n} = 0$$

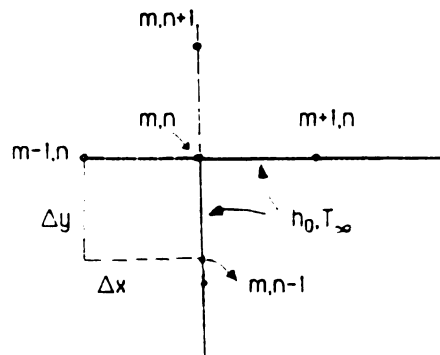


Figure 1 --- "90 degree bend with straight boundaries."

CHAPTER II

Formulation of the Problem

2.1 Coordinate System

Let us assume the plate is of constant thickness $2a$ and its centerline is given as

$$\hat{R} = X'(S')\hat{i} + Y'(S')\hat{j} \quad (1)$$

Here, X' and Y' are Cartesian coordinates in the directions i and j , respectively. Any point inside the plate wall can then be expressed as

$$\hat{X}' = \hat{R}(S') + \eta'\hat{N}(S') + Z'\hat{K} \quad (2)$$

From the Frenet formulas [8] we find

$$|d\hat{X}'|^2 = (1-K'\eta')^2(dS')^2 + (d\eta')^2 + (dZ')^2 \quad (3)$$

where K' is the curvature and S' , η' , Z' constitute an orthogonal intrinsic coordinate system as shown in Figure 2. The boundary is described by $\eta' = \pm a$.

Let the temperature on both sides of the plate be maintained at a constant value to produce the following boundary conditions.

$$\eta' = a, T = T_0, \text{ and } \eta' = -a, T = T_1 \quad (4)$$

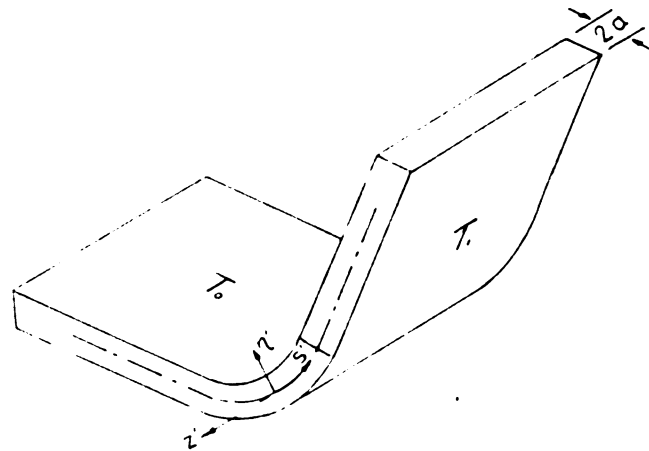


Figure 2. --The Bent Plate and (η, s) Coordinate System.

Introducing the appropriate scale factors, Laplace's equation becomes

$$\begin{aligned} & \left(\frac{1}{1-K'\eta'} \right) \left\{ \frac{\partial}{\partial S'} \left(\frac{1}{1-K'\eta'} \cdot \frac{\partial T}{\partial S'} \right) + \right. \\ & \left. \frac{\partial}{\partial \eta'} \left[(1-K'\eta') \frac{\partial T}{\partial \eta'} \right] \right\} = 0 \end{aligned} \quad (5)$$

where we will normalize all lengths by 'a' and drop the primes. The temperature field is normalized by introducing the following:

$$T = (T_0 - T_1)X(\eta) + T_1 \quad (6)$$

By using this representation of the temperature field, we reduce the problem to one where we are solving for the function $X(\eta)$. Equation (5) thus becomes:

$$\frac{\partial}{\partial S} \left(\frac{1}{1-K\eta} \cdot \frac{\partial X}{\partial S} \right) + \frac{\partial}{\partial \eta} \left[(1-K\eta) \frac{\partial X}{\partial \eta} \right] = 0 \quad (7)$$

with the boundary conditions

$$\eta = 1, X = 1; \eta = -1, X = 0; -\infty < S < \infty \quad (8)$$

If the curvature K is constant (which corresponds to a circular bend), the solution is found to be:

$$X = \ln\left(\frac{1-K\eta}{1+K}\right) / \ln\left(\frac{1-K}{1+K}\right) \quad (9)$$

This result agrees with Reference [3].

2.2 Transformation to a Round Corner

For an arbitrary curvature $K(S)$, a perturbation solution is possible when the plate width is small compared to the local radius of curvature, i.e.,

$$K'a \equiv K(S) \equiv \epsilon k(S) \ll 1 \quad (10)$$

where ϵ is a small number defined as $\max |K'a|$ and $k(S)$ is of order unity. Let us concentrate on the geometry shown in Figure 2. The plate consists of two semi-infinite straight sections joined by a circular section. The curvature of the centerline is given as

$$k(S) = \begin{cases} 1 & |S| \leq b \\ 0 & |S| > b \end{cases} \quad (11)$$

Substituting Equations (10) and (11) into (7), the final governing equations are:

$$\begin{aligned} (\partial^2 X / \partial \eta^2) + (\partial^2 X / \partial S^2) &= 0 \\ \text{For } k(S) &= 0, \text{ or } |S| > b \end{aligned} \quad (12)$$

$$\begin{aligned} (\partial^2 X / \partial S^2) + \epsilon(\epsilon\eta - 1)(\partial X / \partial \eta) + \\ (1 - \epsilon\eta)^2 (\partial^2 X / \partial \eta^2) &= 0 \\ \text{For } k(S) &= 1, \text{ or } |S| \leq b \end{aligned} \quad (13)$$

Note that the first equation describes straight segments while the latter refers to the curved section.

2.3 Parameters

The radius of curvature (R') and the thickness of the plate (2a) are dimensional quantities. The dimensionless parameters are $2b$ and θ , respectively, where $2b$ is the total length of bend and which is divided into two equal parts b by the η -axis. Facing the arc $2b$ is the angle θ . See Figure 3f.

Equation (14) indicates how ϵ is defined and equation (15) is the relation among these parameters.

$$\epsilon = a/R \quad (14)$$

$$\theta = 2b\epsilon \quad (15)$$

A value of zero for b indicates that the plate is completely straight without any bend. If $\epsilon = 0.0$, then according to Equation (14), R tends toward infinity which, in turn, indicates that the plate is again straight. This is because "a" can not be equal to zero.

Figures 3, 4 and 5 show how the different values of these parameters affect the shape of the bent plate because they are related to one another according to equations (14) and (15).

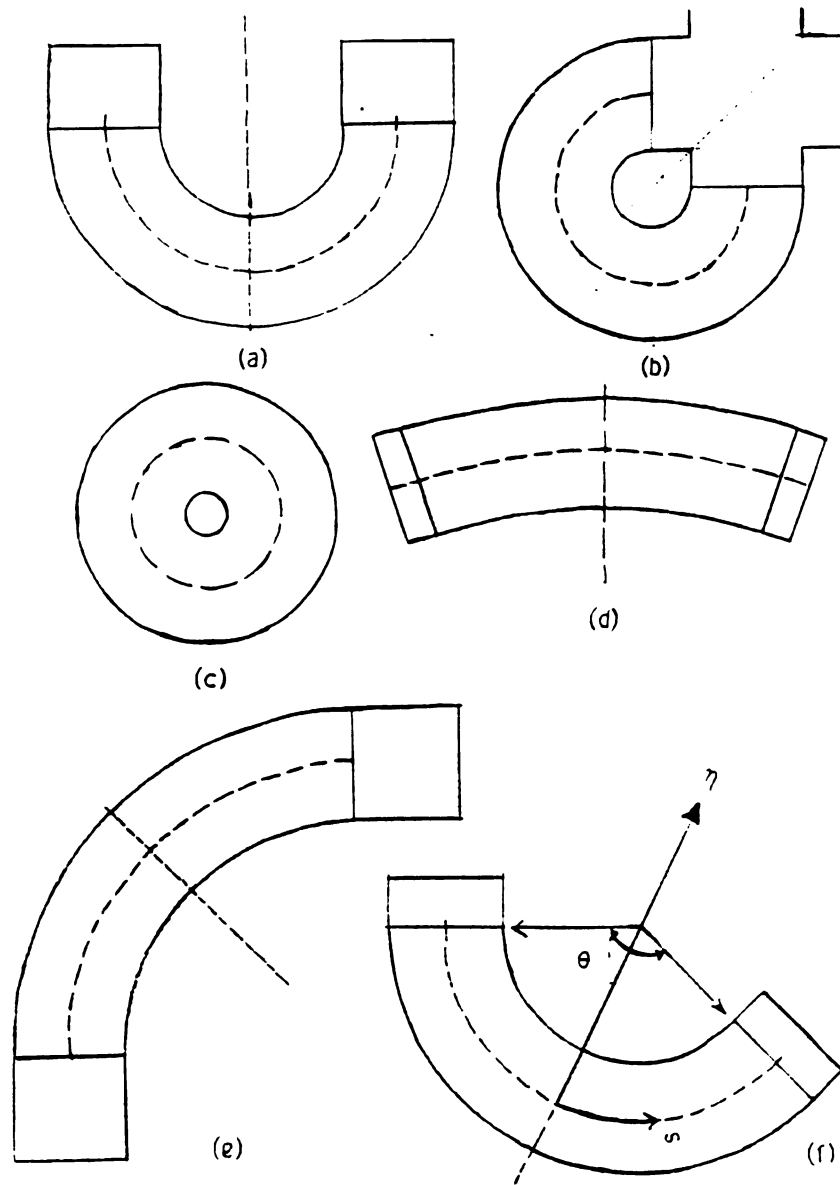


Figure 3.--Bent Plates with $b=4.0$ and (a) $\theta=\pi$, (b) $\theta=3\pi/2$, (c) $\theta=2\pi$, (d) $\theta=\pi/4$, (e) $\theta=\pi/2$ and (f) $\theta=3\pi/4$

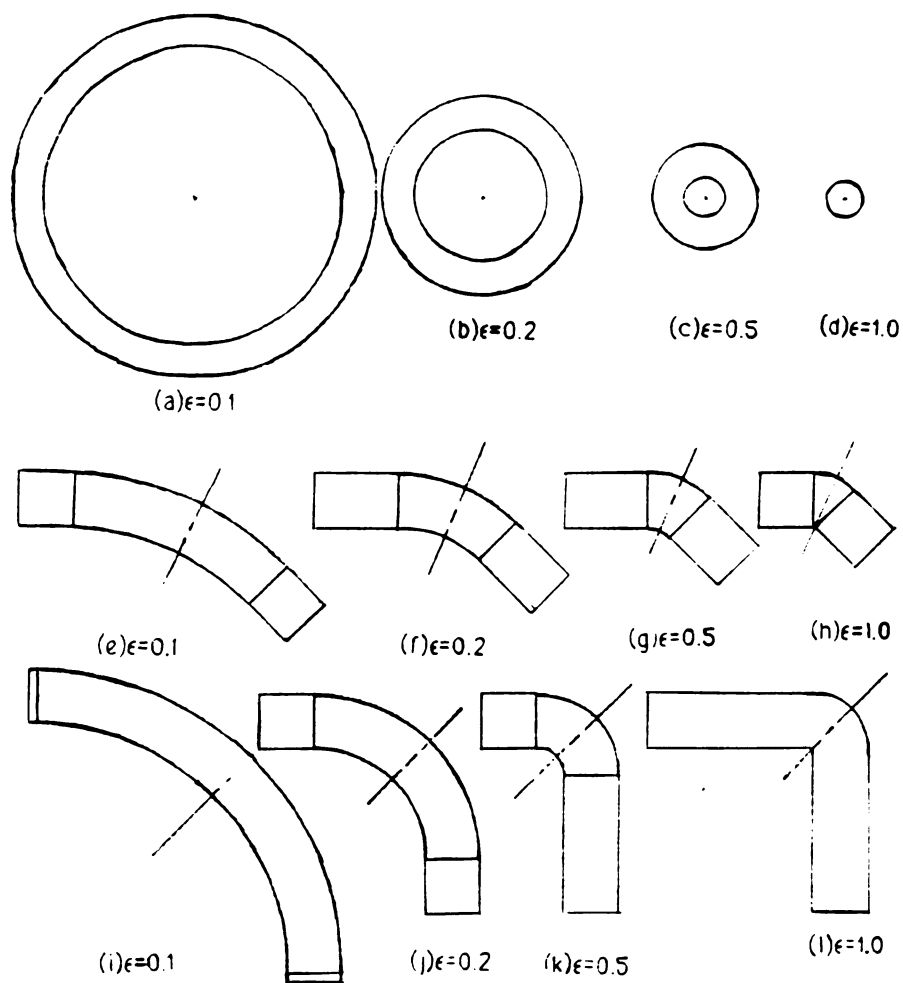


Figure 4.-- Bent Plates With $\theta=2\pi$ for a,b,c and d $\theta=\pi/2$ for i,j,k and l $\theta=\pi/4$ for e,f,g and h.

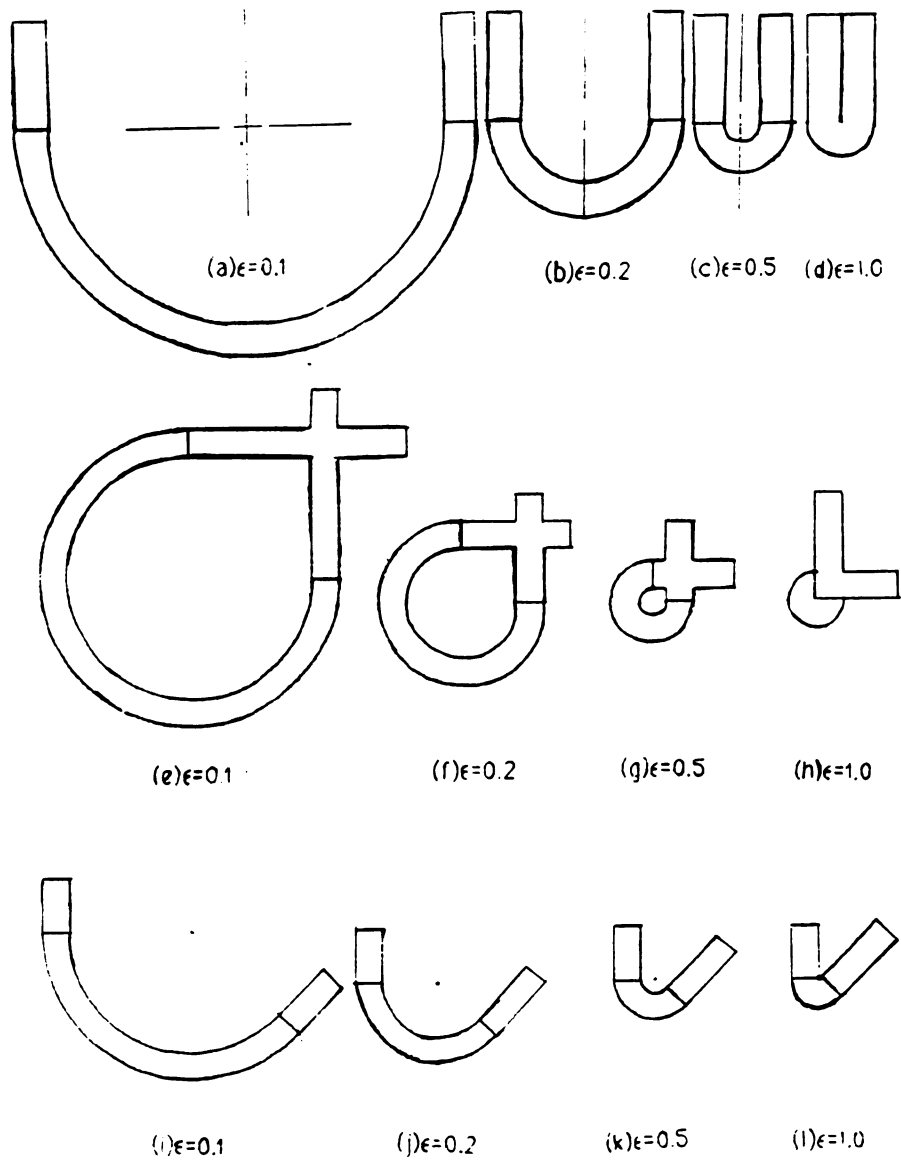


Figure 5.--Bent Plates When $\theta=\pi$ for a, b, c and d, $\theta=3\pi/2$ for e, f, g and h, $\theta=3\pi/4$ for i, j, k and l

CHAPTER III

Finite Difference Method

We will utilize the fact that the plate is symmetric about the η -axis to reduce our computational effort. This will be used throughout the rest of the formulation.

3.1 Boundary Conditions

The inner surface, which corresponds to $\eta = +1$, has the temperature of $X = 1$. On the outer surface, $\eta = -1$ and $X = 0$. Along the η -axis (corresponding to $S = 0$), symmetry will be used which yields an adiabatic surface with $\partial X / \partial S \approx 0$. In the segments far away from the bend, the temperature is assumed to approach the flat plate solution. In other words, it changes linearly from $X = 1$ to $X = 0$ because: (i) there is steady-state condition, and (ii) no curvature effects are involved in the geometry. Figure 6 shows these conditions.

Thus, two different forms of the governing differential equations are used: one in the curved and the other one in the straight sections of plate. If the curved and straight segments are separated as shown in Figure 6, along the border line, not only the temperature distribution is the same for both segments but the heat

coming in s-direction from one side must go out through the other side. If at a point (η, s) along this line the temperatures are called X_1 and X_2 for the curved and straight segments respectively, then the boundary conditions along the line separating the two parts would be:

$$X_1 = X_2 \quad (16)$$

$$(\partial X_1 / \partial S) = (\partial X_2 / \partial S) \quad (17)$$

Figure 6 shows all the boundary conditions involved. To clearly illustrate the two domains (straight and curved sections), the whole plate is shown as two separate pieces. The cut is at the shared boundary between the two segments.

3.2 Formulation for the Interior Nodes

Equations (12) and (13) are converted into finite difference form using a "Central-Difference" representation and taking h and l as mesh lengths along η and S -axis, respectively [2].

$$\begin{aligned} & \frac{1}{l^2} (X_{i,j+1} - 2X_{i,j} + X_{i,j-1}) + \epsilon (\epsilon h i - 1) \frac{X_{i+1,j} - X_{i-1,j}}{2h} \\ & + (1 - \epsilon h i)^2 \frac{1}{h^2} (X_{i+1,j} - 2X_{i,j} + X_{i-1,j}) = 0 \end{aligned}$$

$$\text{For } k = 1 \quad (18)$$

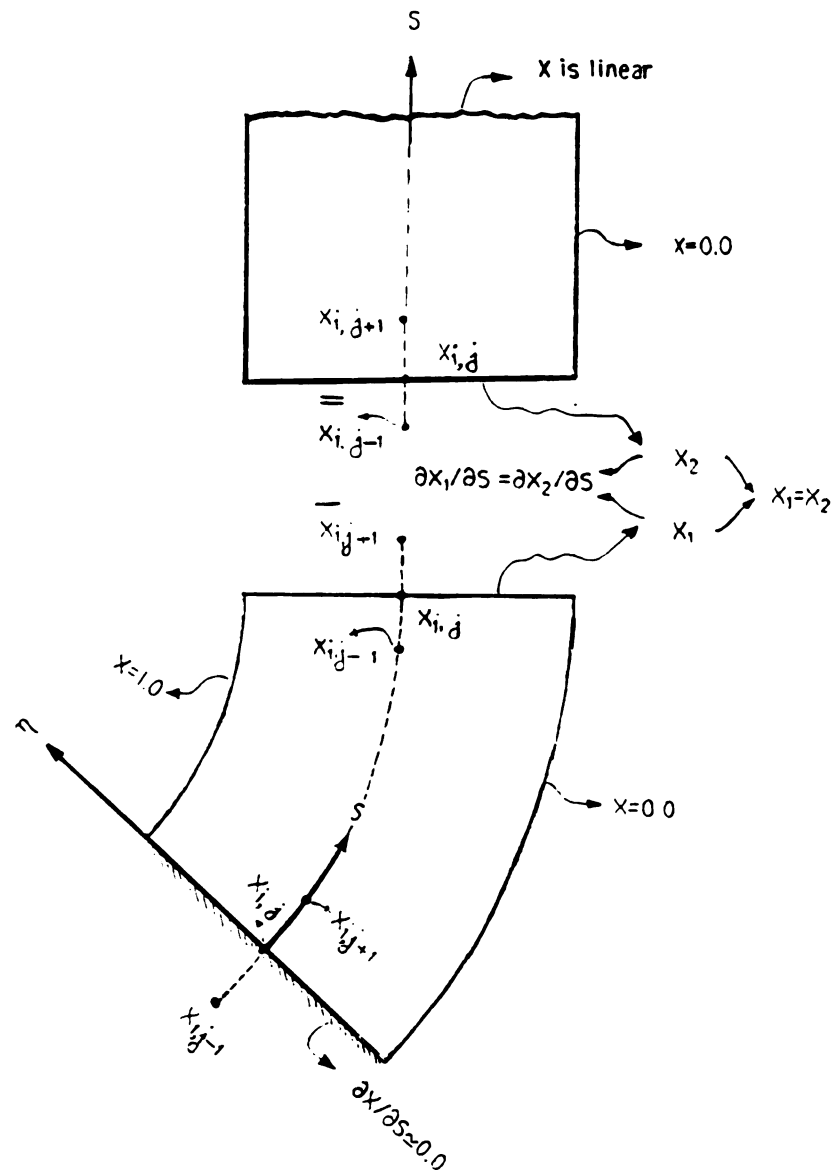


Figure 6.—Representation of Boundaries and Boundary Conditions.

$$\frac{1}{l^2}(x_{i,j+1} - 2x_{i,j} + x_{i,j-1}) +$$

$$\frac{1}{h^2}(x_{i+1,j} - 2x_{i,j} + x_{i-1,j}) = 0$$

$$\text{For } k = 0 \quad (19)$$

The following relations were used in equations (18) and (19):

$$\eta = hi \quad (20)$$

$$s = lj \quad (21)$$

$$\partial x / \partial \eta = (x_{i+1,j} - x_{i-1,j}) / 2h \quad (22)$$

$$\partial^2 x / \partial s^2 = \frac{1}{l^2}(x_{i,j+1} - 2x_{i,j} + x_{i,j-1}) \quad (23)$$

$$\partial^2 x / \partial \eta^2 = \frac{1}{h^2}(x_{i+1,j} - 2x_{i,j} + x_{i-1,j}) \quad (24)$$

If

$$r = l^2/h^2 \quad (25)$$

then Equations (18) and (19) become

$$\begin{aligned}
& (-2r(1-\epsilon hi)^2 - 2)X_{i,j} + (r(1-\epsilon hi)^2 + \frac{1^2 \epsilon (\epsilon hi - 1)}{2h})X_{i+1,j} \\
& + (r(1-\epsilon hi)^2 - \frac{1^2 \epsilon (\epsilon hi - 1)}{2h})X_{i-1,j} \\
& + X_{i,j+1} + X_{i,j-1} = 0
\end{aligned}$$

$$\text{when } k = 1 \quad (26)$$

$$\begin{aligned}
& (-2r-2)X_{i,j} + rX_{i+1,j} + rX_{i-1,j} + \\
& X_{i,j+1} + X_{i,j-1} = 0
\end{aligned}$$

$$\text{when } k = 0 \quad (27)$$

To further simplify the equations, the following substitutions are made:

$$-2r(1-\epsilon hi)^2 - 2 = E(i) \quad (28)$$

$$r(1-\epsilon hi)^2 + \frac{1^2 \epsilon (\epsilon hi - 1)}{2h} = F(i) \quad (29)$$

$$r(1-\epsilon hi)^2 - \frac{1^2 \epsilon (\epsilon hi - 1)}{2h} = G(i) \quad (30)$$

The final form of Equations (12) and (13) for the interior nodes in the curved and straight sections thus take the following form:

$$\begin{aligned}
& E(i)X_{i,j} + F(i)X_{i+1,j} + G(i)X_{i-1,j} + \\
& X_{i,j-1} + X_{i,j+1} = 0 \\
& \text{when } k = 1
\end{aligned} \tag{31}$$

$$\begin{aligned}
& (-2r-2)X_{i,j} + rX_{i+1,j} + rX_{i-1,j} + \\
& X_{i,j-1} + X_{i,j+1} = 0 \\
& \text{when } k = 0
\end{aligned} \tag{32}$$

Equation (31) holds for interior points when $|S| < b$, $k = 1$ and Equation (32) holds for interior points having $|S| > b$, $k = 0$.

3.3 Formulation for the Boundary Conditions

a) The first boundary to be discussed is the adiabatic surface corresponding to the symmetry boundary.

$$\partial X / \partial S \approx 0 \tag{33}$$

$$\frac{X_{i,j+1} - X_{i,j-1}}{2\Delta} = 0 \tag{34}$$

$$X_{i,j+1} = X_{i,j-1} \tag{35}$$

If $X_{i,j-1}$ is cancelled between Equations (35) and (31), the equation which must be used for the adiabatic boundary is:

$$E(i)X_{i,j} + F(i)X_{i+1,j} + G(i)X_{i-1,j} + 2X_{i,j+1} = 0 \quad (36)$$

b) As discussed earlier, the boundary separating the curved and straight parts uses continuity arguments. Equations (16) and (17) are the boundary conditions

$$(\partial X_1 / \partial s) = (\partial X_2 / \partial S) \quad (37)$$

and by using a central difference, Equation (37) becomes

$$\frac{\bar{X}_{i,j+1} - X_{i,j-1}}{2l} = \frac{X_{i,j+1} - \bar{\bar{X}}_{i,j-1}}{2l} \quad (38)$$

$$\bar{X}_{i,j+1} - X_{i,j-1} = X_{i,j+1} - \bar{\bar{X}}_{i,j-1} \quad (39)$$

where \bar{X} and $\bar{\bar{X}}$ are two fictitious points as shown in Figure 6. Assuming fictitious points is the common approach used in a finite difference method to handle the nodes located on boundaries. The bars over X are used to make a distinction between the two fictitious nodes.

Equations (31) and (32) along this line become:

$$E(i)X_{i,j} + F(i)X_{i+1,j} + G(i)X_{i-1,j} + \bar{X}_{i,j+1} + X_{i,j-1} = 0 \quad (40)$$

$$(-2r-2)X_{i,j} + rX_{i+1,j} + rX_{i-1,j} + X_{i,j+1} + \bar{\bar{X}}_{i,j-1} = 0 \quad (41)$$

Since $X_{i,j}$ is the same for both Equations (40) and (41), the condition $X_1 = X_2$ has already been incorporated into these equations. If \bar{X} and $\bar{\bar{X}}$ are now eliminated from equations (39), (40) and (41), the following equation results which is applicable only for the line separating two segment domains.

$$\begin{aligned} Z(i)X_{i,j} + (F(i)+r)X_{i+1,j} + (G(i)+r)X_{i-1,j} \\ + 2X_{i,j-1} + 2X_{i,j+1} = 0 \end{aligned} \quad (42)$$

where

$$Z(i) = E(i) - 2r - 2 \quad (43)$$

All of the applicable equations for different sections can be summarized below:

- 1) Equation (31)--Only for the points inside the curved segment.
- 2) Equation (32)--Only for the points inside the straight part.
- 3) Equation (36)--Along the adiabatic surface corresponding to the line of symmetry.
- 4) Equation (42)--Along the line separating the curved and straight segments of the plate.

3.4 Node Generation

Along the η -axis, 11 points are uniformly distributed. Along S-axis, 22 points are considered. The

plate is thus divided into small meshes with a total of nodes 242. Figure 7 shows this division. This number represents a compromise between the increased accuracy offered by more nodes and the constraints of memory size and execution time. In dimensionless terms, the mesh lengths are:

$$h = 2/10 = .2 \quad (44)$$

$$l = b/6 \quad (45)$$

3.5 Computer Program

The system of equations for the nodal temperatures are obtained from Equations (31), (32), (36) and (42) and can be formulated as $AX = B$. The computer program is organized in several routines. The first creates the matrices A and B. A call is then made to the IMSL libraries to solve $AX = B$ using the subroutine "LEQTIF." Figure 8 shows the flow chart of the program. The program is included in an appendix.

3.6 Temperature Distribution along η -axis

The conduction equation across a cylinder [6] is

$$q = \frac{2\pi kL (T_i - T_o)}{\ln(R_o/R)} \quad (46)$$

From this equation, the temperature distribution becomes

$$T = T_i - \frac{T_i - T_o}{\ln(R_o/R_i)} \ln(R/R_i) \quad (47)$$

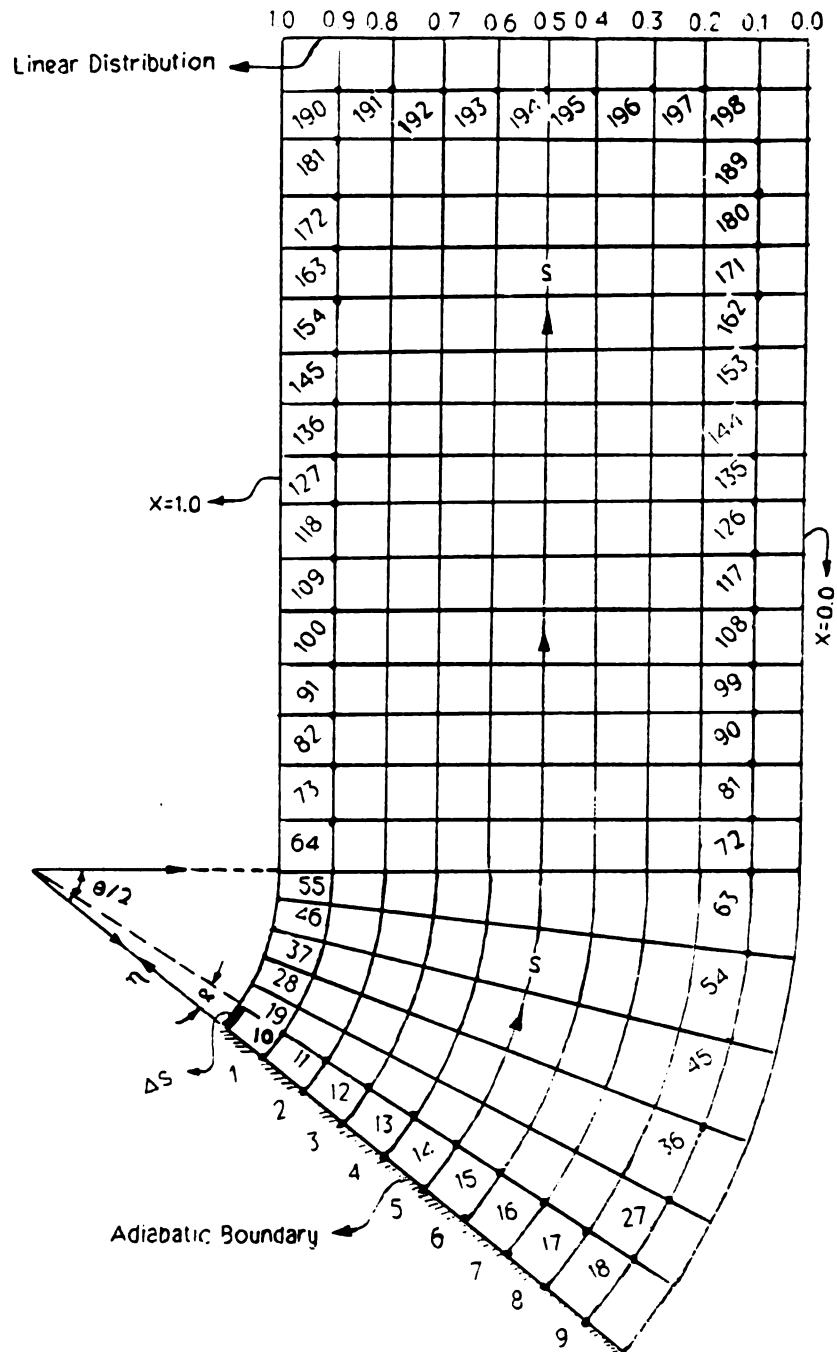


Figure 7.--Representation of Nodes

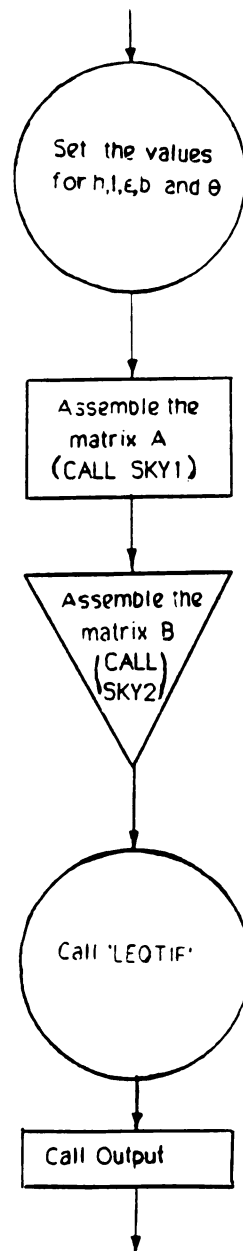


Figure 8.--- Computer Flowchart

Substituting Equation (6) into (48)

$$X = 1 - \frac{\ln(R/R_i)}{\ln(R_o/R_i)} \quad (48)$$

which is the dimensionless temperature along the η -axis for a cylinder. The linear distribution of the dimensionless temperature along the η -axis with respect to R is

$$X = \frac{R_o - R}{R_o - R_i} \quad (49)$$

The difference (dimensionless) between these two distributions is:

$$\Delta X = \frac{R_o - R}{R_o - R_i} - 1 + \frac{\ln(R/R_i)}{\ln(R_o/R_i)} \quad (50)$$

and this difference is maximum at the point where

$$R = \frac{R_o - R_i}{\ln(R_o/R_i)} \quad (51)$$

When the plate thickness is small compared to the radius of the centerline R_o , the maximum temperature deficiency in this case is located at:

$$R = \frac{R_o + R_i}{2} \quad (52)$$

In his work, C.Y. Wang [4] refers to this point as "The worst temperature deficiency" which occurs at $S = 0$, $\eta = 0$ along the η -axis only for small values of ε . Figure

9 shows that the temperature deficiency along η -axis can be closely approximated as a parabolic distribution when the plate thickness is small compared to R_c . Table 26 shows the location and value of maximum temperature deficiency along η -axis for different values of ε and θ .

3.7 Heat-transfer and Shape Factor

In this section, Figure 7 will be very helpful to and in the understanding of the equations and proofs. From Equation (15), the radius of curvature for the center-line where $\eta = 0$ is

$$R'_c = \frac{2ba}{\theta} \quad (53)$$

$$R'_i = R'_c - a = \frac{2ba}{\theta} - a = a((2b-\theta)/\theta) \quad (54)$$

where R'_i is the radius of curvature for the interior curved boundary, and "a" is half of the plate thickness. The following shows the calculation of the length of each division along the η -axis and the interior boundary. See Figure 7 for better understanding of the following calculations, which are divided into three parts.

- 1) The dimensional mesh length along the η -axis

$$\Delta\eta' = \frac{2a}{10} = .2a \quad (55)$$

- 2) The dimensional mesh length on the interior boundary in the curved segment

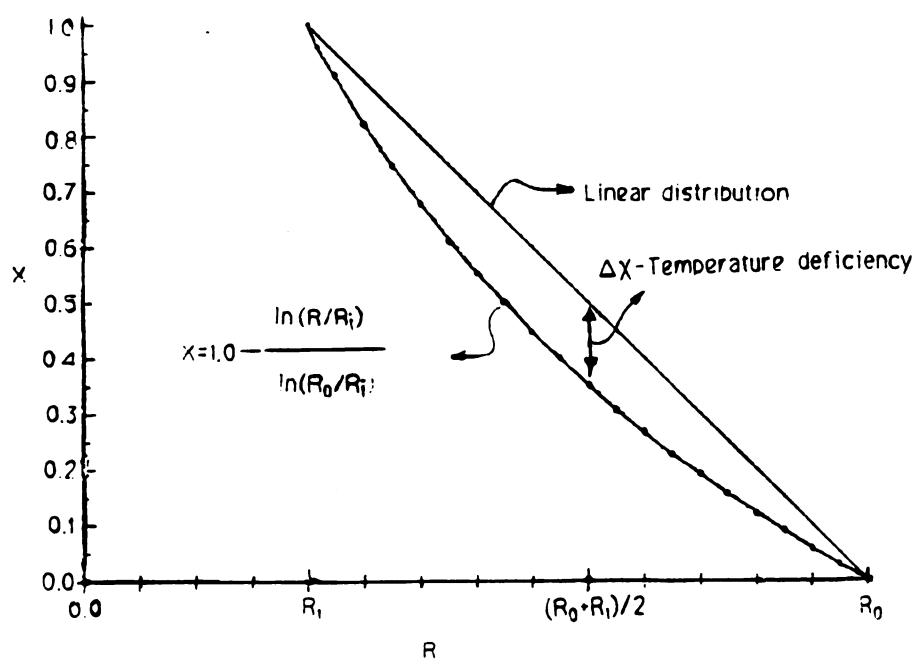


Figure 9.--Showing the temperature deficiency along η axis

$$\alpha = \frac{\theta/2}{6.0} = \theta/12 \quad (56)$$

$$\Delta S' = R'_i \alpha = \frac{a(2b-\theta)}{12} \quad (57)$$

3) The dimensional mesh length along the interior boundary in the straight segment of the plate

$$\Delta S' = \frac{ba}{6.0} \quad (58)$$

The heat conduction equation is [6]

$$q = \sum_{i=1}^{22} KA(\Delta T/\Delta \eta') \quad (59)$$

From Equation (6), the temperature difference between every two nodes on the same line is

$$\Delta T = (T_o - T_1) \Delta X = (\Delta T_{\text{overall}})(\Delta X) = (\Delta T_o)(\Delta X) \quad (60)$$

Considering a unit depth in z' -direction and dividing Equation (59) into two parts in order to take care of the fact that the divisions along the interior boundary are not the same in the curved and straight segments of the plate and also substituting Equation (60) for ΔT , the result is

$$q = \sum_{i=1}^6 Ka \left(\frac{2b-\theta}{12} \right) (1) \left(\frac{\Delta T_o \Delta X}{0.2a} \right) + \sum_{i=7}^{22} K \left(\frac{ba}{6.0} \right) (1) \left(\frac{\Delta T_o \Delta X}{0.2a} \right) \quad (62)$$

or

$$\frac{q}{K\Delta T_o} = \left(\frac{2b-\theta}{2.4}\right) \sum_{i=1}^6 \Delta X_i + \frac{b}{1.2} \sum_{i=7}^{22} \Delta X_i \quad (63)$$

The shape factor S is related to q according to [6]

$$q = KS\Delta T_o \quad (64)$$

or

$$\frac{q}{K\Delta T_o} = S \quad (65)$$

The temperatures along the line next to the interior boundary at the indicated nodes are tabulated in Tables 22 through 26 and the values of heat transfer in the form of $\frac{q}{K\Delta T_o}$ which is equal to the shape factor S , are shown in Table 25.

3.8 Isotherms

For each different shape, the isotherms can be found by linear interpolation for the temperatures between adjacent nodes to obtain the desired temperature. As an example, isotherms are shown on Figure 10 when $\theta = \pi/2$ and $b = 4$. For other shapes, isotherms can be found in a similar way. The location of the intersections of isotherms with the η -axis are also shown in Figure 24 when $\theta = \pi/2$. This picture illustrates the deviation of these isotherms from the linear distribution for a flat plate with the same thickness.

3.9 Error Estimate

By considering two nodes at $\eta = +1/3$ and $\eta = -1/3$ along the η -axis and another one at $s = b/2$ along the s -axis, different mesh lengths h and l were considered to see how many digits are valid and can be trusted. Results showed that only three digits are valid. Table 27 shows the results and Figure 25 through 27 are the plots of these temperatures verses h , h^2 , l and l^2 . These figures show that the temperature varies linearly when they are plotted verses h^2 and l^2 .

The error is due to two factors, the first is the truncation error in central-difference formulation in the finite difference method and the second is the computer round off.

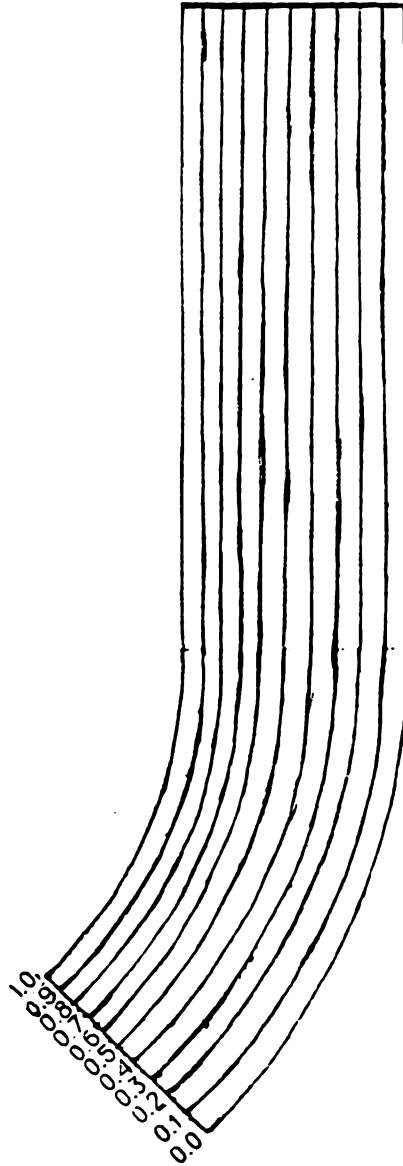


Figure 10.-- The isotherms when $\theta = \pi/2$ and $b = 4.0$

CHAPTER IV

Results and Conclusions

4.1 Numerical Results

Temperature distributions were calculated for selected values of θ , b and ϵ using a finite difference method expressed by Equations (31), (32), (36) and (42).

Tables 1 through 18 include all the results for different values of these parameters. The results confirm the statements made by C.Y. Wang [4] concerning the analytical results. The results indicate that the temperatures at any given (η, S) in the vicinity of the bend are less than their corresponding values for the linear distribution in a flat plate with the same thickness. This is attributed to the difference in areas between the inner surface and outer surface. Since the heat transfer rate is proportional to this area, the area difference results in the isotherms being closer together near the inner surface. See Figure 10.

For a given angle of bend and bend length b (or curvature), the temperatures along the centerline are less than the linear value of 0.5, and the minimum temperature along this line is located at $S = 0$, $\eta = 0$ since this

point is the furthest point from the straight segments. Figures 11 and 13 through 17 show the change of temperatures along the S-axis and Tables 2 and 14 through 18 contain the numerical values for different values of parameters.

The temperatures in the vicinity of the bend have decreased from their corresponding linear values even for the adjacent straight sections. The temperatures do not relax back to the linear temperature distribution until one reaches a certain penetration depth along S-axis. This is due to the effect of the bend on the neighboring parts of straight sections. Table 19 shows the penetration depth for different values of parameters.

As b decreases, the temperatures at any given (η, S) in the vicinity of the bend increase due to the fact that the bend length is being slowly reduced which, in turn, makes the plate behave more like a flat plate. In the limit, as $b \rightarrow 0$ the temperature deficiency decreases and temperatures reach their linear values.

Along the η -axis or $S = 0$, the temperatures are less than their corresponding linear values and as discussed in Section 3.6, when the plate thickness is small compared to radius of curvature R_C , the temperature deficiency is parabolic along this axis. The maximum temperature deficiency in this case occurs at $S = 0$, $\eta = 0$. This is an approximation which loses its validity as ϵ

increases to larger values, (i.e., the plate thickness is not small compared to the radius of curvature R_c). Table 26 shows the maximum temperature deficiency along η -axis and its location.

As ϵ decreases for a given value of b , the temperatures along η -axis are increased. This can be seen in Figures 13 to 17. As θ decreases (which means the angle of bend increases and the plate becomes flatter), the temperatures approach the linear values. The temperature distributions are shown in Figure 18 through 22. Tables 1 and 3 through 13 also contain additional results.

For a given ϵ , the shape factors and the heat transfer are increased as the angle of the bend increases (θ decreases). For a given angle of the bend (or θ), the shape factors and heat transfer are decreased as ϵ increases. See Table 25.

4.2 Conclusion

Based on the results obtained and the discussion in the previous section, it can be concluded that:

- 1) The temperatures are decreased in the vicinity of the bend when compared with the linear distribution of a flat plate with the same thickness.
- 2) For a given θ (or angle of the bend) and bend length b (or curvature) the temperatures

along the S-axis are less than the linear value of .5 for the centerline.

- 3) The maximum temperature deficiency along the S-axis is observed at $\eta = 0, S = 0$.
- 4) The maximum temperature deficiency along any line parallel to S-axis is located at $(\eta, 0)$.
- 5) Moving along the S-axis, the linear temperature distribution is observed in the straight segments up to a penetration depth that depends on $2b$ and θ .
- 6) The temperature deficiency from linear distribution along η -axis is parabolic when $\epsilon \ll 1$.
- 7) As b decreases, the temperatures for any given (η, S) in the vicinity of the bend increase and as $b \rightarrow 0$ they reach the values of temperature distribution in a flat plate with the same thickness.
- 8) For a given angle θ , as ϵ increases (b decreases) the temperatures at any given point (η, S) in the vicinity of the bend decrease.
- 9) For a given ϵ , as θ increases, the heat transfer and shape factors increase.
- 10) For a given θ (or angle of the bend) as ϵ increases, the heat transfer and shape factors decrease.
- 11) The results are accurate only to three significant digits.

It is clear that the effect of curvature (bend) cannot be ignored on the temperature distribution along a bend plate. In his work, C.Y. Wang [4] assumed that the plate thickness is very small when compared with the radius of curvature of centerline, (i.e., $\epsilon \ll 1$). The numerical results not only confirm the results of analytical solution, but also relaxes the restriction of being a lot smaller than unity which is imposed upon the analytical solution.

Table 1: Dimensionless temperatures along η -axis when
 $b = 2.0$.

η	$\theta=\pi/4$	$\theta=\pi/4$	$\theta=3\pi/4$	$\theta=\pi$
-1	0.000	0.000	0.000	0.000
-4/5	0.084	0.071	0.059	0.048
-3/5	0.172	0.147	0.123	0.101
-2/5	0.262	0.227	0.193	0.159
-1/5	0.356	0.313	0.270	0.224
0.0	0.453	0.405	0.354	0.298
1/5	0.554	0.504	0.448	0.384
2/5	0.658	0.611	0.554	0.484
3/5	0.767	0.727	0.676	0.607
4/5	0.881	0.856	0.821	0.766
1	1.00	1.00	1.00	1.00

Table 2: Dimensionless temperatures along s-axis when
b = 2.0.

s/l $l=1/3$	$\theta=\pi/4$	$\theta=\pi/2$	$\theta=3\pi/4$	$\theta=\pi$
0	0.453	0.405	0.354	0.299
1	0.453	0.405	0.355	0.300
2	0.454	0.408	0.359	0.306
3	0.456	0.412	0.366	0.316
4	0.460	0.419	0.377	0.333
5	0.466	0.431	0.396	0.358
6	0.475	0.451	0.425	0.398
7	0.485	0.470	0.454	0.438
8	0.491	0.482	0.472	0.462
9	0.495	0.489	0.483	0.478
10	0.497	0.494	0.490	0.487
11	0.498	0.496	0.494	0.492
12	0.499	0.498	0.496	0.495
13	0.499	0.499	0.448	0.497
14	0.500	0.499	0.499	0.498
15	0.500	0.500	0.499	0.499
16	0.500	0.500	0.500	0.499
17	0.500	0.500	0.500	0.500
18	0.500	0.500	0.500	0.500
19	0.500	0.500	0.500	0.500
20	0.500	0.500	0.500	0.500
21	0.500	0.500	0.500	0.500

Table 3: Dimensionless temperatures along η -axis when $\theta = \pi/4$ and ε varies.

η	$\varepsilon=0.1$	$\varepsilon=0.2$	$\varepsilon=0.5$	$\varepsilon=1.0$
-1	0.000	0.000	0.000	0.000
-4/5	0.091	0.084	0.072	0.066
-3/5	0.185	0.172	0.150	0.139
-2/5	0.280	0.262	0.232	0.219
-1/5	0.376	0.355	0.320	0.307
0	0.475	0.452	0.413	0.402
1/5	0.576	0.553	0.513	0.505
2/5	0.678	0.658	0.620	0.616
3/5	0.783	0.767	0.733	0.736
4/5	0.891	0.881	0.858	0.865
1	1.00	1.00	1.00	1.00

Table 4: Dimensionless temperatures along s-axis when $\theta = \pi/2$ and ε varies.

η	$\varepsilon=0.1$	$\varepsilon=0.2$	$\varepsilon=0.5$	$\varepsilon=1.0$
-1	0.000	0.000	0.000	0.000
-4/5	0.091	0.084	0.066	0.054
-3/5	0.184	0.170	0.137	0.113
-2/5	0.280	0.260	0.213	0.179
-1/5	0.376	0.353	0.295	0.253
0	0.475	0.450	0.384	0.337
1/5	0.576	0.551	0.481	0.431
2/5	0.678	0.6555	0.588	0.530
3/5	0.783	0.765	0.707	0.665
4/5	0.890	0.880	0.842	0.815
1	1.000	1.000	1.00	1.00

Table 5: Dimensionless temperatures along η -axis when $\theta = 3\pi/4$ and ε varies.

η	$\varepsilon=0.1$	$\varepsilon=0.2$	$\varepsilon=0.5$	$\varepsilon=1.0$
-1	0.000	0.000	0.000	0.000
-4/5	0.091	0.0836	0.064	0.0456
-3/5	0.185	0.170	0.132	0.097
-2/5	0.280	0.260	0.206	0.154
-1/5	0.376	0.353	0.287	0.219
0	0.475	0.450	0.374	0.292
1/5	0.576	0.550	0.471	0.378
2/5	0.678	0.655	0.578	0.479
3/5	0.783	0.765	0.698	0.602
4/5	0.890	0.880	0.837	0.761
1	1.00	1.00	1.00	1.00

Table 6: Dimensionless temperatures along s-axis when $\theta = \pi$ and ε varies.

η	$\varepsilon=0.1$	$\varepsilon=0.2$	$\varepsilon=0.5$	$\varepsilon=1.0$
-1	0.000	0.000	0.000	0.000
-4/5	0.091	0.084	0.063	0.040
-3/5	0.185	0.170	0.131	0.085
-2/5	0.280	0.260	0.204	0.136
-1/5	0.376	0.353	0.284	0.193
0	0.475	0.450	0.371	0.260
1/5	0.576	0.550	0.467	0.337
2/5	0.678	0.655	0.574	0.431
3/5	0.783	0.765	0.696	0.549
4/5	0.890	0.880	0.835	0.711
1.0	1.00	1.00	1.00	1.00

Table 7: Dimensionless temperatures along s-axis when $\theta = 3\pi/2$ and ε varies.

η	$\varepsilon=0.1$	$\varepsilon=0.2$	$\varepsilon=0.5$	$\varepsilon=1.0$
-1	0.000	0.000	0.000	0.000
-4/5	0.091	0.084	0.063	0.033
-3/5	0.185	0.170	0.130	0.071
-2/5	0.280	0.260	0.203	0.112
-1/5	0.376	0.353	0.283	0.160
0	0.475	0.450	0.370	0.216
1/5	0.576	0.550	0.466	0.283
2/5	0.678	0.655	0.573	0.366
3/5	0.783	0.765	0.694	0.474
4/5	0.890	0.880	0.834	0.635
1	1.00	1.00	1.00	1.00

Table 8: Dimensionless temperatures along η -axis when $\theta = 2\pi$ and ε varies.

η	$\varepsilon=0.1$	$\varepsilon=0.2$	$\varepsilon=0.5$
-1	0.000	0.000	0.000
-4/5	0.091	0.084	0.063
-3/5	0.185	0.170	0.130
-2/5	0.280	0.260	0.203
-1/5	0.376	0.353	0.282
0	0.475	0.450	0.369
1/5	0.576	0.550	0.465
2/5	0.678	0.655	0.572
3/5	0.783	0.765	0.694
4/5	0.890	0.880	0.834
1	1.00	1.00	1.00

Table 9: Dimensionless temperatures along η -axis when $\theta = \pi/4$ and b varies.

η	$b=0.5$	$b=1.0$	$b=2.0$	$b=3.0$
-1	0.000	0.000	0.000	0.000
-4/5	0.068	0.075	0.084	0.089
-3/5	0.142	0.155	0.172	0.180
-2/5	0.222	0.240	0.262	0.274
-1/5	0.309	0.329	0.356	0.369
0	0.402	0.423	0.453	0.468
1/5	0.502	0.523	0.554	0.568
2/5	0.611	0.629	0.658	0.672
3/5	0.727	0.742	0.767	0.778
4/5	0.854	0.865	0.881	0.887
1	1.00	1.00	1.00	1.00

Table 10: Dimensionless temperatures along η -axis when $\theta = \pi/2$ and b varies.

η	$b=1.0$	$b=2.0$	$b=3.0$	$b=4.0$
-1	0.000	0.000	0.000	0.000
-4/5	0.057	0.071	0.079	0.084
-3/5	0.119	0.147	0.162	0.171
-2/5	0.188	0.227	0.249	0.261
-1/5	0.263	0.313	0.339	0.354
0	0.347	0.405	0.435	0.451
1/5	0.440	0.504	0.535	0.551
2/5	0.546	0.611	0.641	0.656
3/5	0.667	0.727	0.753	0.766
4/5	0.811	0.856	0.872	0.880
1	1.00	1.00	1.00	1.00

Table 11: Dimensionless temperatures along η -axis when $\theta = 3\pi/4$ and b varies.

η	$b=2.0$	$b=3.0$	$b=4.0$	$b=5.0$
-1	0.000	0.000	0.000	0.000
-4/5	0.059	0.070	0.077	0.081
-3/5	0.123	0.145	0.157	0.165
-2/5	0.193	0.224	0.242	0.253
-1/5	0.270	0.309	0.331	0.345
0	0.3540	0.401	0.426	0.440
1/5	0.4480	0.499	0.526	0.541
2/5	0.554	0.606	0.632	0.647
3/5	0.676	0.724	0.746	0.758
4/5	0.821	0.854	0.868	0.875
1	1.00	1.00	1.00	1.00

Table 12: Dimensionless temperatures along η -axis when $\theta = \pi$ and b varies.

	b=2.0	b=4.0	b=6.0	b=8.0
-1	0.000	0.000	0.000	0.000
-4/5	0.048	0.070	0.079	0.084
-3/5	0.101	0.144	0.162	0.171
-2/5	0.159	0.226	0.248	0.261
-1/5	0.224	0.308	0.339	0.354
0	0.299	0.400	0.434	0.451
1/5	0.384	0.498	0.534	0.551
2/5	0.485	0.605	0.640	0.656
3/5	0.607	0.723	0.753	0.766
4/5	0.766	0.853	0.872	0.880
1	1.00	1.00	1.00	1.00

Table 13: Dimensionless temperatures along s-axis when $\theta = 3\pi/2$ and b varies.

η	b=3.0	b=4.0	b=5.0	b=6.0
-1	0.000	0.000	0.000	0.000
-4/5	0.045	0.057	0.048	0.070
-3/5	0.095	0.119	0.134	0.144
-2/5	0.150	0.187	0.209	0.223
-1/5	0.212	0.261	0.289	0.308
0	0.283	0.344	0.378	0.399
1/5	0.366	0.437	0.474	0.498
2/5	0.465	0.543	0.582	0.605
3/5	0.588	0.666	0.702	0.723
4/5	0.752	0.815	0.840	0.854
1	1.00	1.00	1.00	1.00

Table 14: Dimensionless temperatures along s-axis when
 $\theta = \pi/4$.

s/l	$\varepsilon=0.1$ $l=\pi/4.8$	$\varepsilon=0.2$ $l=\pi/9.6$	$\varepsilon=0.5$ $l=\pi/2.4$	$\varepsilon=1.0$ $l=\pi/48.0$
0	0.475	0.452	0.413	0.402
1	0.475	0.453	0.414	0.403
2	0.475	0.454	0.416	0.404
3	0.476	0.456	0.420	0.408
4	0.477	0.459	0.426	0.412
5	0.480	0.465	0.434	0.418
6	0.488	0.475	0.443	0.425
7	0.495	0.485	0.453	0.433
8	0.498	0.491	0.462	0.440
9	0.499	0.494	0.469	0.450
10	0.500	0.497	0.474	0.452
11	0.500	0.498	0.479	0.458
12	0.500	0.499	0.483	0.463
13	0.500	0.499	0.486	0.468
14	0.500	0.500	0.489	0.472
15	0.500	0.500	0.491	0.476
16	0.500	0.500	0.493	0.480
17	0.500	0.500	0.495	0.484
18	0.500	0.500	0.496	0.487
19	0.500	0.500	0.497	0.490
20	0.500	0.500	0.498	0.494
21	0.500	0.500	0.499	0.497

Table 15: Dimensionless temperatures along s-axis when
 $\theta = \pi/2$.

s/l	$\varepsilon=0.1$ $l=\pi/2.4$	$\varepsilon=0.2$ $l=\pi/4.8$	$\varepsilon=0.5$ $l=\pi/12.0$	$\varepsilon=1.0$ $l=\pi/24.$
0	0.475	0.450	0.384	0.337
1	0.475	0.450	0.385	0.338
2	0.475	0.450	0.388	0.343
3	0.475	0.451	0.394	0.350
4	0.475	0.453	0.403	0.361
5	0.477	0.459	0.417	0.375
6	0.488	0.475	0.437	0.393
7	0.498	0.490	0.457	0.412
8	0.500	0.496	0.471	0.428
9	0.500	0.499	0.481	0.441
10	0.500	0.500	0.487	0.452
11	0.500	0.500	0.492	0.461
12	0.500	0.500	0.494	0.468
13	0.500	0.500	0.496	0.474
14	0.500	0.500	0.498	0.479
15	0.500	0.500	0.498	0.483
16	0.500	0.500	0.499	0.487
17	0.500	0.500	0.499	0.490
18	0.500	0.500	0.500	0.492
19	0.500	0.500	0.500	0.494
20	0.500	0.500	0.500	0.496
21	0.500	0.500	0.500	0.498

Table 16: Dimensionless temperatures along s-axis when
 $\theta = 3\pi/4$.

s/l	$\varepsilon=0.1$ $l=3\pi/4.8$	$\varepsilon=0.2$ $l=3\pi/9.6$	$\varepsilon=0.5$ $l=3\pi/24.0$	$\varepsilon=1.0$ $l=3\pi/48$
0	0.475	0.450	0.374	0.292
1	0.475	0.450	0.375	0.294
2	0.475	0.450	0.378	0.301
3	0.475	0.450	0.383	0.311
4	0.475	0.451	0.392	0.327
5	0.476	0.456	0.408	0.350
6	0.488	0.475	0.437	0.379
7	0.499	0.494	0.465	0.410
8	0.500	0.498	0.481	0.432
9	0.500	0.500	0.489	0.450
10	0.500	0.500	0.494	0.463
11	0.500	0.500	0.497	0.473
12	0.500	0.500	0.498	0.480
13	0.500	0.500	0.499	0.485
14	0.500	0.500	0.499	0.489
15	0.500	0.500	0.500	0.492
16	0.500	0.500	0.500	0.494
17	0.500	0.500	0.500	0.496
18	0.500	0.500	0.500	0.497
19	0.500	0.500	0.500	0.498
20	0.500	0.500	0.500	0.499
21	0.500	0.500	0.500	0.499

Table 17: Dimensionless temperatures along s-axis when
 $\theta = \pi$.

s/l	$\varepsilon=0.1$ $l=\pi/1.2$	$\varepsilon=0.2$ $l=\pi/2.4$	$\varepsilon=0.5$ $l=\pi/6.0$	$\varepsilon=1.0$ $l=\pi/12.0$
0	0.475	0.450	0.371	0.260
1	0.475	0.450	0.372	0.262
2	0.475	0.450	0.373	0.270
3	0.475	0.450	0.374	0.282
4	0.4750	0.450	0.385	0.302
5	0.476	0.454	0.402	0.331
6	0.488	0.475	0.437	0.372
7	0.499	0.496	0.471	0.413
8	0.500	0.499	0.487	0.412
9	0.500	0.500	0.494	0.461
10	0.500	0.500	0.497	0.474
11	0.500	0.500	0.499	0.482
12	0.500	0.500	0.499	0.488
13	0.500	0.500	0.500	0.492
14	0.500	0.500	0.500	0.495
15	0.500	0.500	0.500	0.497
16	0.500	0.500	0.500	0.498
17	0.500	0.500	0.500	0.499
18	0.500	0.500	0.500	0.499
19	0.500	0.500	0.500	0.499
20	0.500	0.500	0.500	0.500
21	0.500	0.500	0.500	0.500

Table 18: Dimensionless temperatures along s-axis when
 $\theta = 3\pi/2$.

s/l	$\epsilon=0.1$ $l=3\pi/2.4$	$\epsilon=0.2$ $l=3\pi/4.8$	$\epsilon=0.5$ $l=3\pi/12.0$	$\epsilon=1.0$ $l=3\pi/24.$
0	0.475	0.450	0.370	0.216
1	0.475	0.450	0.370	0.219
2	0.475	0.450	0.370	0.228
3	0.475	0.450	0.372	0.243
4	0.475	0.450	0.377	0.268
5	0.475	0.452	0.393	0.3064
6	0.488	0.475	0.437	0.366
7	0.500	0.498	0.480	0.425
8	0.500	0.500	0.494	0.458
9	0.500	0.500	0.498	0.477
10	0.500	0.500	0.499	0.488
11	0.500	0.500	0.500	0.493
12	0.500	0.500	0.500	0.496
13	0.500	0.500	0.500	0.498
14	0.500	0.500	0.500	0.499
15	0.500	0.500	0.500	0.499
16	0.500	0.500	0.500	0.500
17	0.500	0.500	0.500	0.500
18	0.500	0.500	0.500	0.500
19	0.500	0.500	0.500	0.500
20	0.500	0.500	0.500	0.500
21	0.500	0.500	0.500	0.500

Table 19: The dimensionless penetration depth along s-axis to reach the linear values for flat plate.

θ	$\varepsilon=0.1$	$\varepsilon=0.2$	$\varepsilon=0.5$	$\varepsilon=1.0$
$\pi/4$	9.16	7.53	3.27	1.83
$\pi/2$	14.4	9.82	6.54	3.66
$3\pi/4$	19.6	12.8	8.25	5.50
π	26.2	14.4	8.90	7.33
$3\pi/2$	35.3	63495	11.8	9.82

Table 20: The dimensionless temperatures at the indicated nodes when $\theta = \pi/4$.

Node	$\varepsilon=0.1$	$\varepsilon=0.2$	$\varepsilon=0.5$	$\varepsilon=1.0$
1	.890	.881	.858	.865
10	.890	.881	.859	.865
19	.890	.881	.860	.866
28	.891	.882	.862	.867
37	.891	.883	.866	.869
46	.892	.886	.870	.872
55	.895	.890	.876	.875
64	.898	.895	.882	.878
73	.899	.897	.886	.880
82	.900	.898	.889	.882
91	.900	.899	.891	.884
100	.900	.899	.893	.886
109	.900	.900	.894	.888
118	.900	.900	.896	.890
127	.900	.900	.896	.891
136	.900	.900	.897	.892
145	.900	.900	.898	.894
154	.900	.900	.898	.895
163	.900	.900	.899	.896
172	.900	.900	.899	.897
181	.900	.900	.899	.898
190	.900	.900	.900	.899

Table 21: The dimensionless temperatures at the indicated nodes when $\theta = \pi/2$.

Node	$\epsilon=0.1$	$\epsilon=0.2$	$\epsilon=0.5$	$\epsilon=1.0$
1	0.890	0.880	0.842	0.815
10	0.890	0.880	0.843	0.816
19	0.890	0.880	0.845	0.819
28	0.890	0.880	0.848	0.825
37	0.891	0.881	0.853	0.833
46	0.891	0.883	0.861	0.843
55	0.895	0.891	0.874	0.855
64	0.899	0.897	0.884	0.866
73	0.900	0.899	0.890	0.874
82	0.900	0.900	0.894	0.879
91	0.900	0.900	0.896	0.884
100	0.900	0.900	0.897	0.887
109	0.900	0.900	0.898	0.890
118	0.900	0.900	0.899	0.892
127	0.900	0.900	0.899	0.893
136	0.900	0.900	0.900	0.895
145	0.900	0.900	0.900	0.896
154	0.900	0.900	0.900	0.897
163	0.900	0.900	0.900	0.898
172	0.900	0.900	0.900	0.898
181	0.900	0.900	0.900	0.899
190	0.900	0.900	0.900	0.900

Table 22: The dimensionless temperatures at the indicated nodes when $\theta = 3\pi/4$.

Node	$\varepsilon=0.1$	$\varepsilon=0.2$	$\varepsilon=0.5$	$\varepsilon=1.0$
1	0.890	0.880	0.837	0.761
10	0.890	0.880	0.837	0.763
19	0.890	0.880	0.839	0.770
28	0.890	0.880	0.842	0.781
37	0.890	0.880	0.847	0.797
46	0.891	0.882	0.856	0.818
55	0.895	0.891	0.874	0.844
64	0.900	0.898	0.888	0.864
73	0.900	0.900	0.894	0.875
82	0.900	0.900	0.897	0.883
91	0.900	0.900	0.898	0.888
100	0.900	0.900	0.899	0.891
109	0.900	0.900	0.899	0.894
118	0.900	0.900	0.900	0.895
127	0.900	0.900	0.900	0.897
136	0.900	0.900	0.900	0.898
145	0.900	0.900	0.900	0.898
154	0.900	0.900	0.900	0.899
163	0.900	0.900	0.900	0.899
172	0.900	0.900	0.900	0.899
181	0.900	0.900	0.900	0.900
190	0.900	0.900	0.900	0.900

Table 23: The dimensionless temperatures at the indicated nodes when $\theta = \pi$.

Node	$\varepsilon=0.1$	$\varepsilon=0.2$	$\varepsilon=0.5$	$\varepsilon=1.0$
1	0.890	0.880	0.835	0.711
10	0.890	0.880	0.836	0.714
19	0.890	0.880	0.836	0.724
28	0.890	0.880	0.839	0.741
37	0.890	0.880	0.843	0.766
46	9.891	0.881	0.853	0.798
55	0.895	0.891	0.874	0.838
64	0.900	0.899	0.890	0.865
73	0.900	0.900	0.896	0.879
82	0.900	0.900	0.898	0.887
91	0.900	0.900	0.899	0.891
100	0.900	0.900	0.900	0.894
109	0.900	0.900	0.900	0.896
118	0.900	0.900	0.900	0.898
127	0.900	0.900	0.900	0.899
136	0.900	0.900	0.900	0.899
145	0.900	0.900	0.900	0.900
154	0.900	0.900	0.900	0.900
163	0.900	0.900	0.900	0.900
172	0.900	0.900	0.900	0.900
181	0.900	0.900	0.900	0.900
190	0.900	0.900	0.900	0.900

Table 24: The dimensionless temperatures at the indicated nodes when $\theta = 3\pi/2$.

Node	$\varepsilon=0.1$	$\varepsilon=0.2$	$\varepsilon=0.5$	$\varepsilon=1.0$
1	0.890	0.880	0.834	0.635
10	0.890	0.880	0.834	0.640
19	0.890	0.880	0.835	0.654
28	0.890	0.880	0.836	0.679
37	0.890	0.880	0.839	0.715
46	0.890	0.881	0.848	0.767
55	0.891	0.891	0.875	0.835
64	0.895	0.900	0.893	0.871
73	0.900	0.900	0.898	0.886
82	0.900	0.900	0.899	0.892
91	0.900	0.900	0.900	0.896
100	0.900	0.900	0.900	0.898
109	0.900	0.900	0.900	0.899
118	0.900	0.900	0.900	0.899
127	0.900	0.900	0.900	0.900
136	0.900	0.900	0.900	0.900
145	0.900	0.900	0.900	0.900
154	0.900	0.900	0.900	0.900
163	0.900	0.900	0.900	0.900
172	0.900	0.900	0.900	0.900
181	0.900	0.900	0.900	0.900
190	0.900	0.900	0.900	0.900

Table 25: The shape factors and heat transfer ($q/K\Delta T_0$).

θ	$\epsilon=0.1$	$\epsilon=0.2$	$\epsilon=0.5$	$\epsilon=1.0$
$\pi/4$	7.19	3.58	1.39	0.581
$\pi/2$	14.4	7.16	2.78	1.18
$3\pi/4$	21.6	10.7	4.17	1.75
π	28.7	14.3	5.56	2.30
$3\pi/2$	43.3	21.5	8.33	3.38

Table 26: The dimensionless maximum temperature deficiencies and their locations along the η -axis.

θ	ε	η	ΔX
$\pi/4$	0.1	0	0.025
	0.2	0	0.048
	0.5	1/5	0.087
	1.0	0	0.098
$\pi/2$	0.1	0	0.025
	0.2	0	0.050
	0.5	1/5	0.119
	1.0	1/5	0.169
$3\pi/4$	0.1	0	0.025
	0.2	0	0.050
	0.5	1/5	0.129
	1.0	1/5	0.222
π	0.1	0	0.025
	0.2	0	0.050
	0.5	1/5	0.133
	1.0	2/5	0.269
$3\pi/2$	0.1	0	0.025
	0.2	0	0.050
	0.5	1/5	0.134
	1.0	2/5	0.334

Table 27: Dimensionless temperatures at two locations
 along η -axis when h varies and at $s = b/2$
 along s -axis when l varies.

η	$h = 1/3$	$h = 1/6$	$h = 1/12$
+1/3	0.62235	0.62226	0.62224
-1/3	0.29263	0.29256	0.29255
s	$l = b/4$	$l = b/8$	$l = b/16$
$b/2$	0.45588	0.45571	0.45568

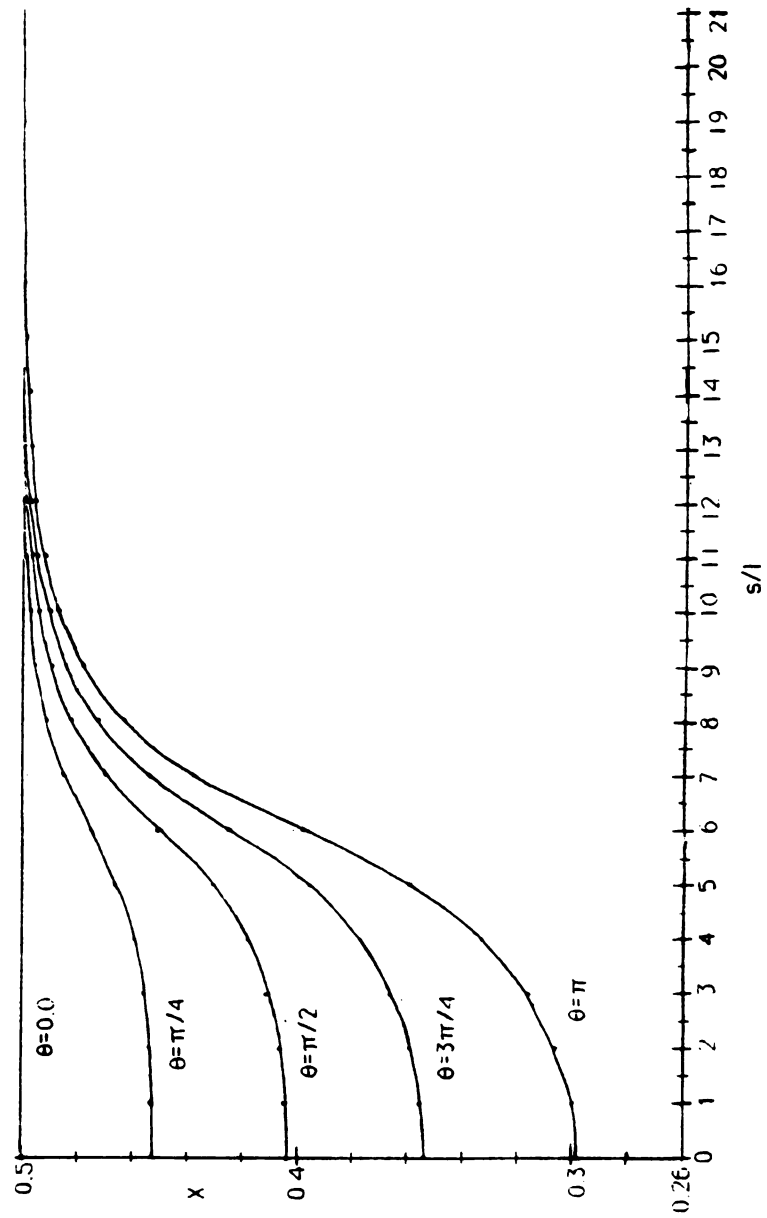


Figure 11.--- Dimensionless Temperatures along S-axis when $b=2.0$

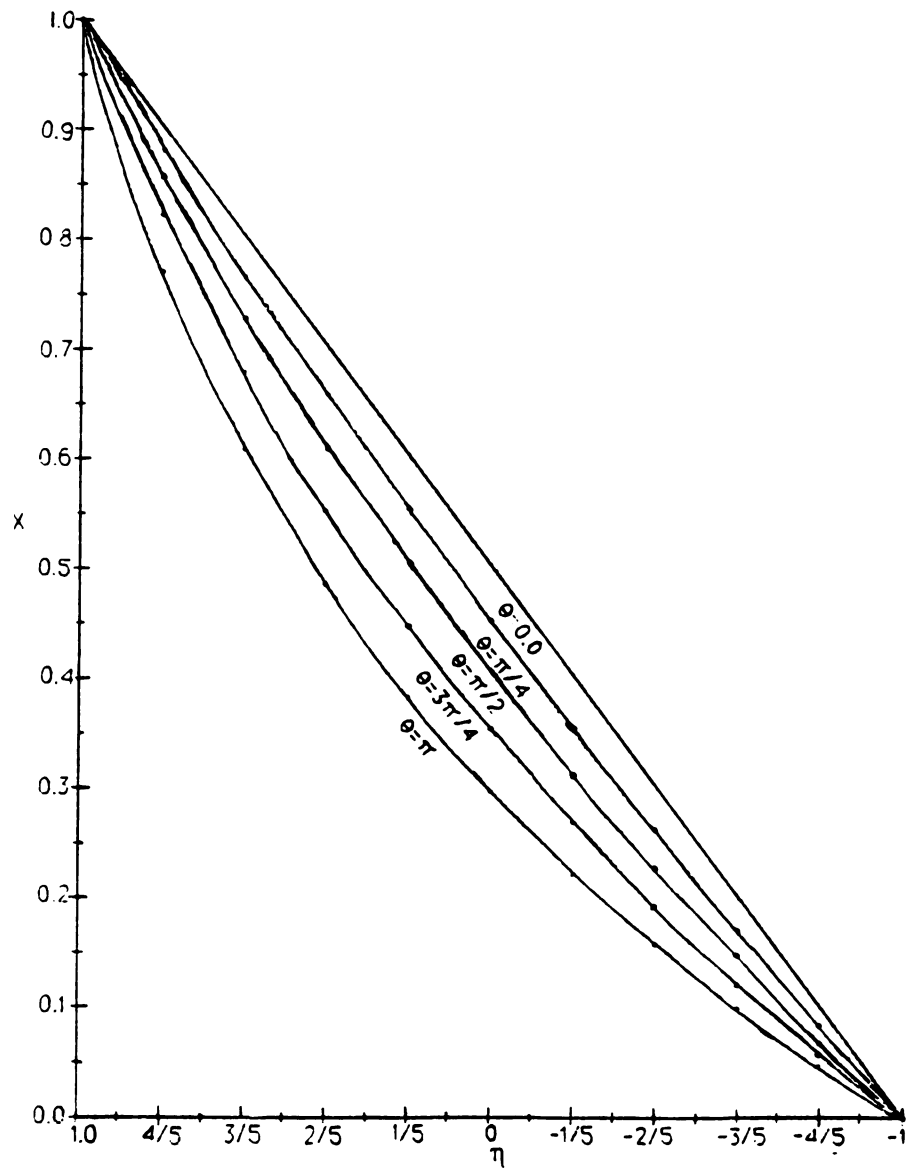


Figure 12.-- Dimensionless Temperatures Along η -axis when $b=2.0$

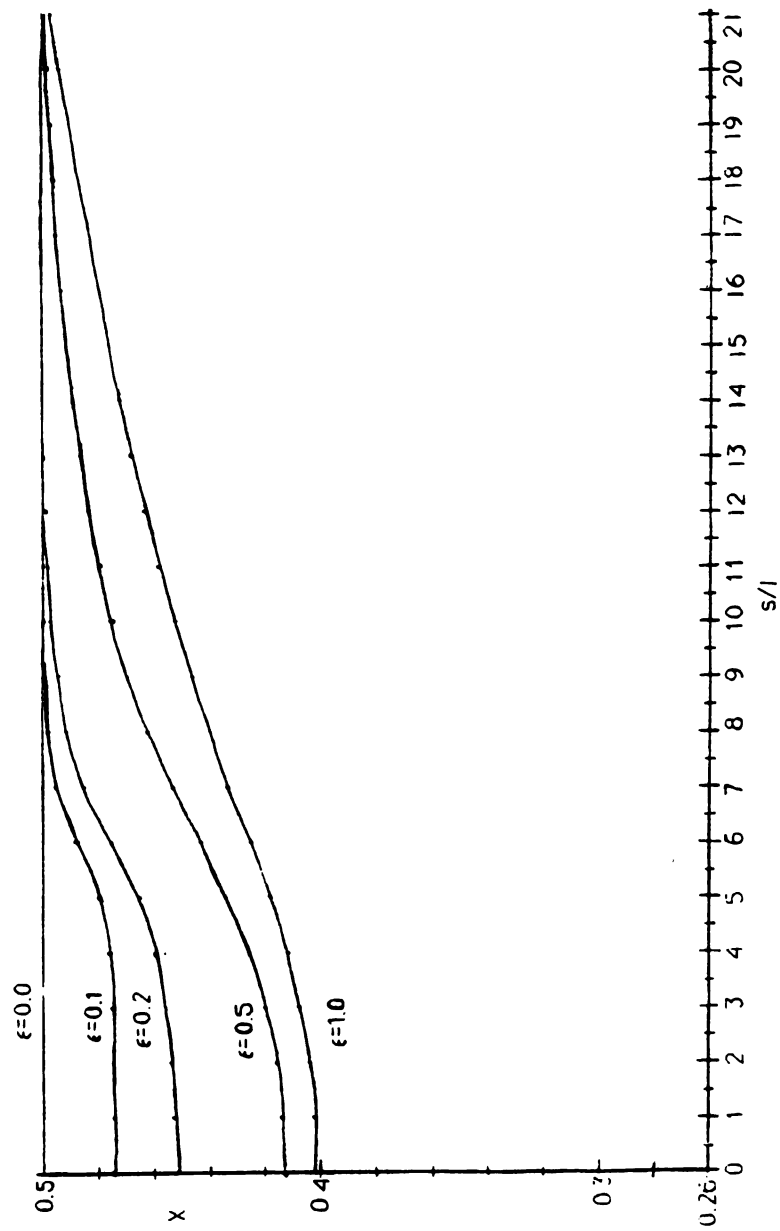


Figure 13. --- Dimensionless Temperatures along S-axis when $\theta = \pi/4$

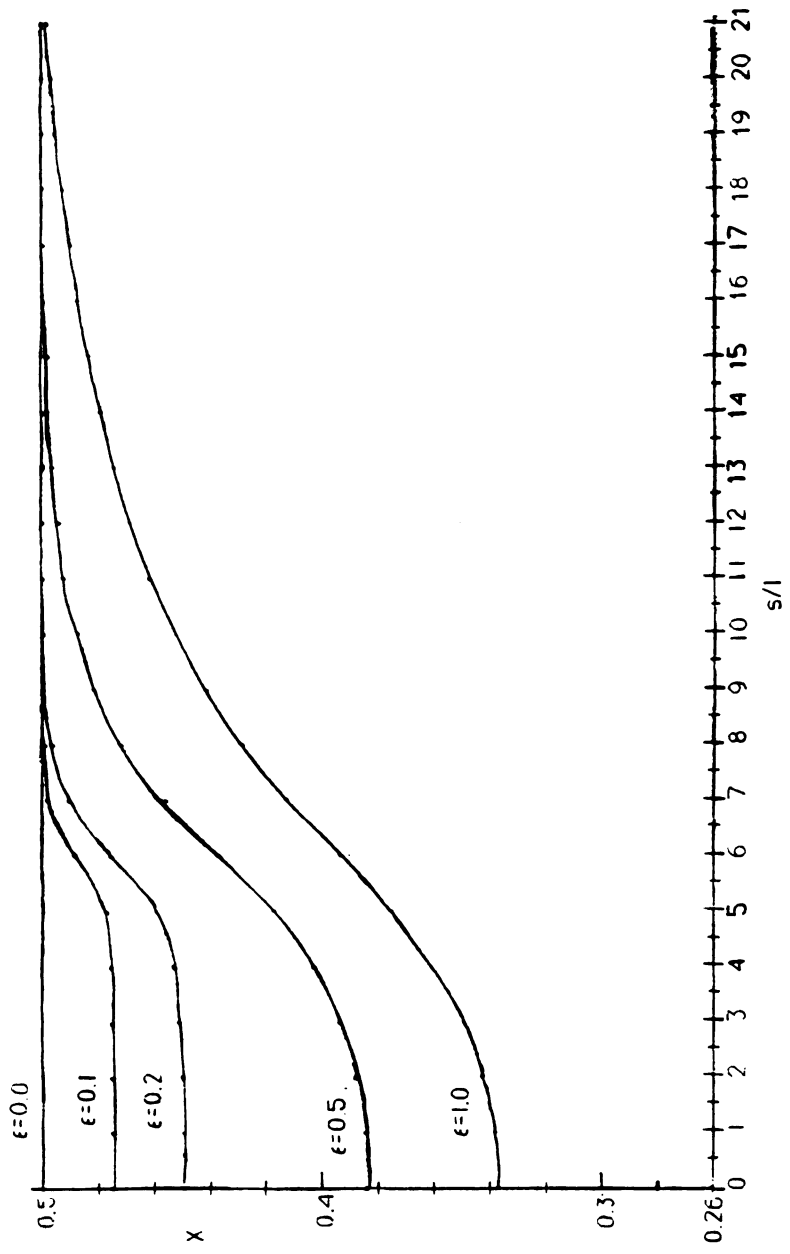


Figure 14. Dimensionless Temperatures along S-axis when $\theta = \pi/2$

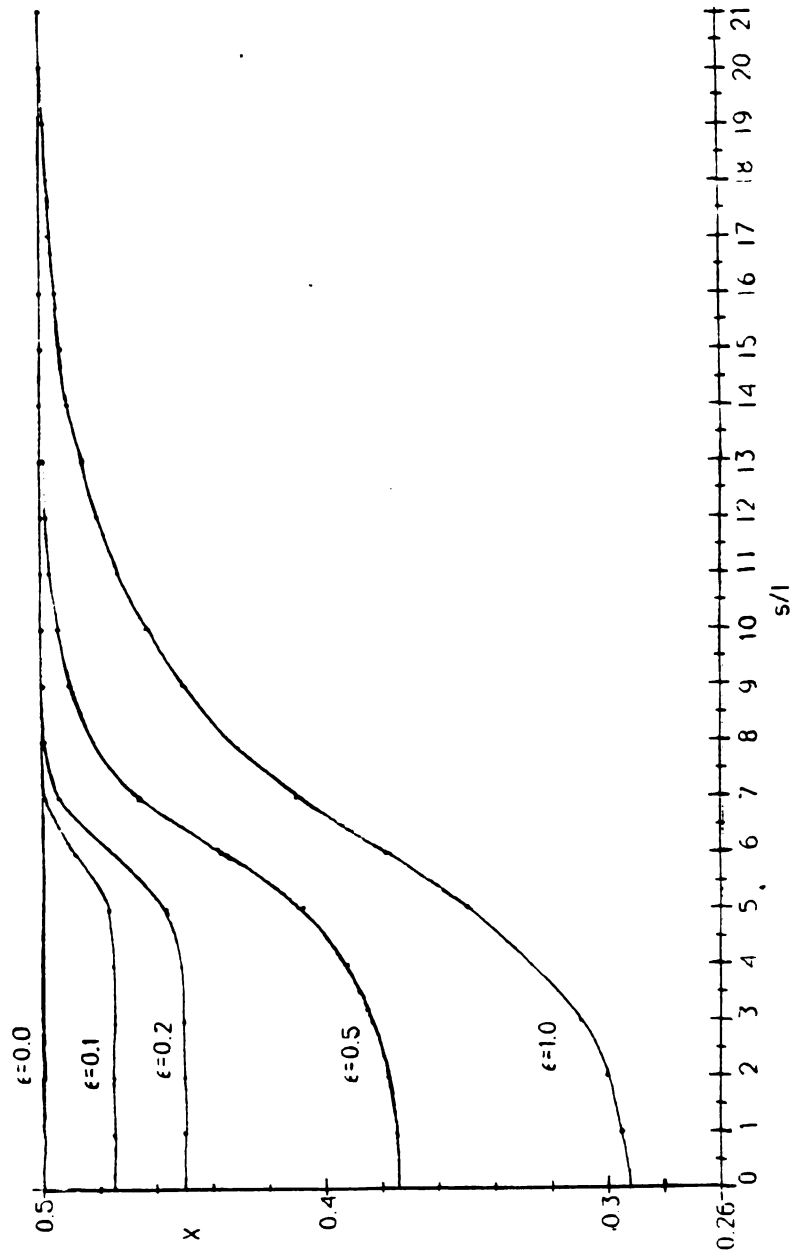


Figure 15. -- Dimensionless Temperatures along S-axis when $\theta = 3\pi/4$

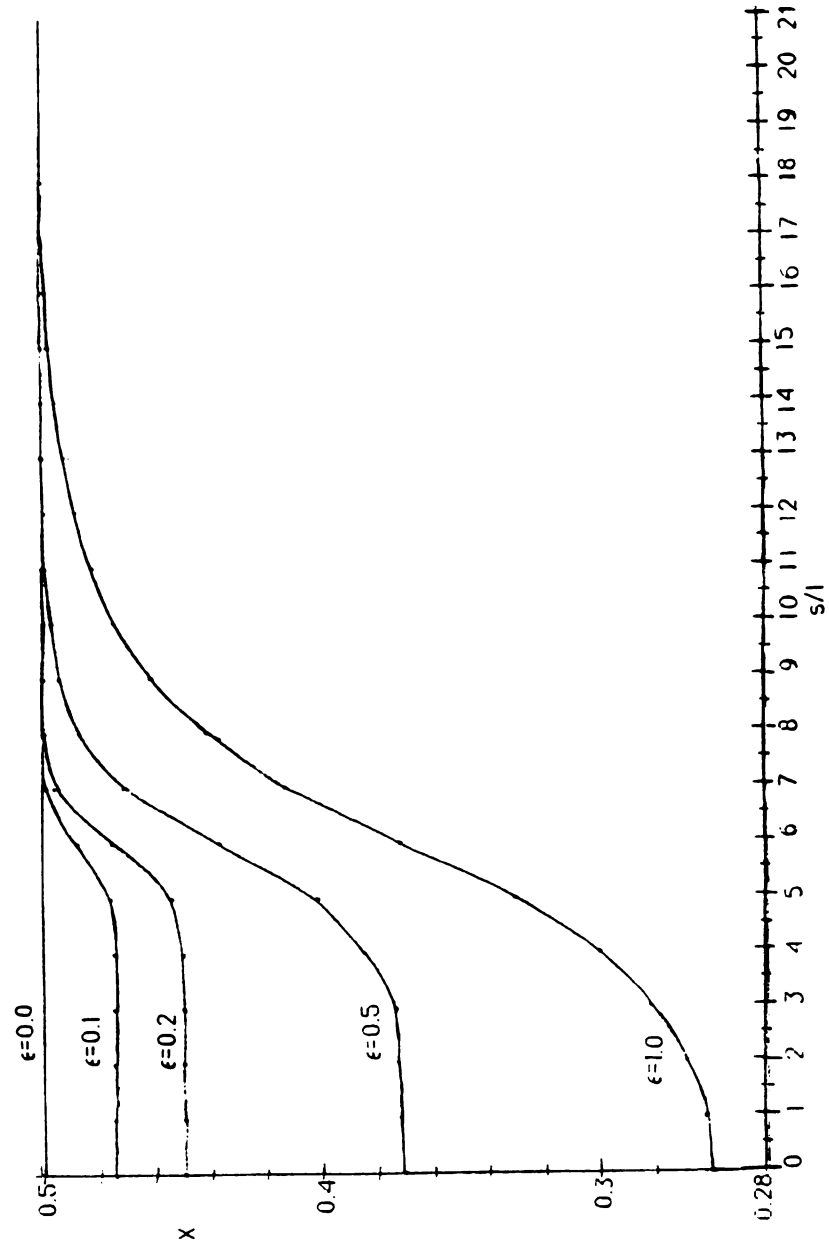


Figure 16.---Dimensionless Temperatures along S-axis when $\theta = \pi$

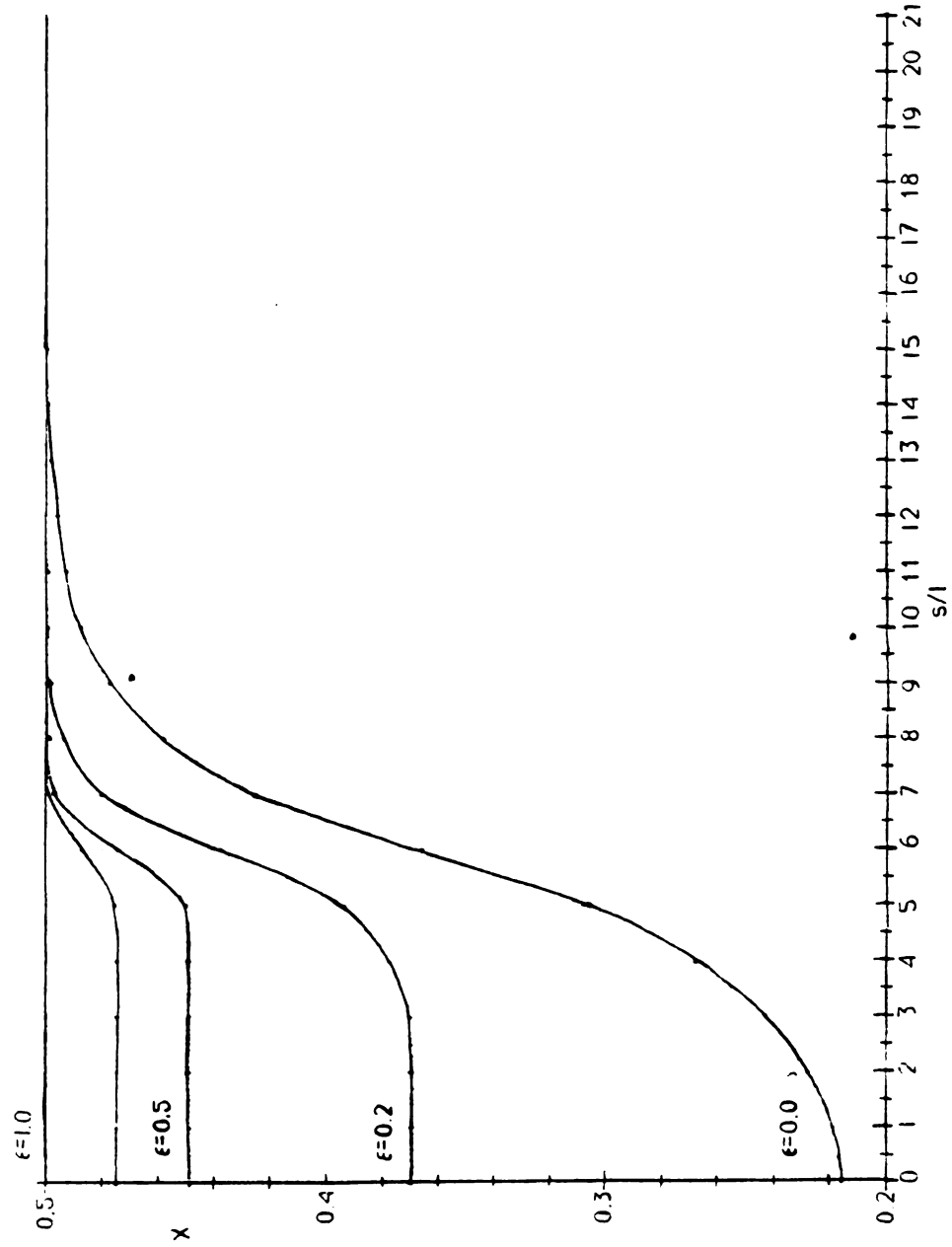


Figure 17.--- Dimensionless Temperatures along S -axis when $\theta=3\pi/2$

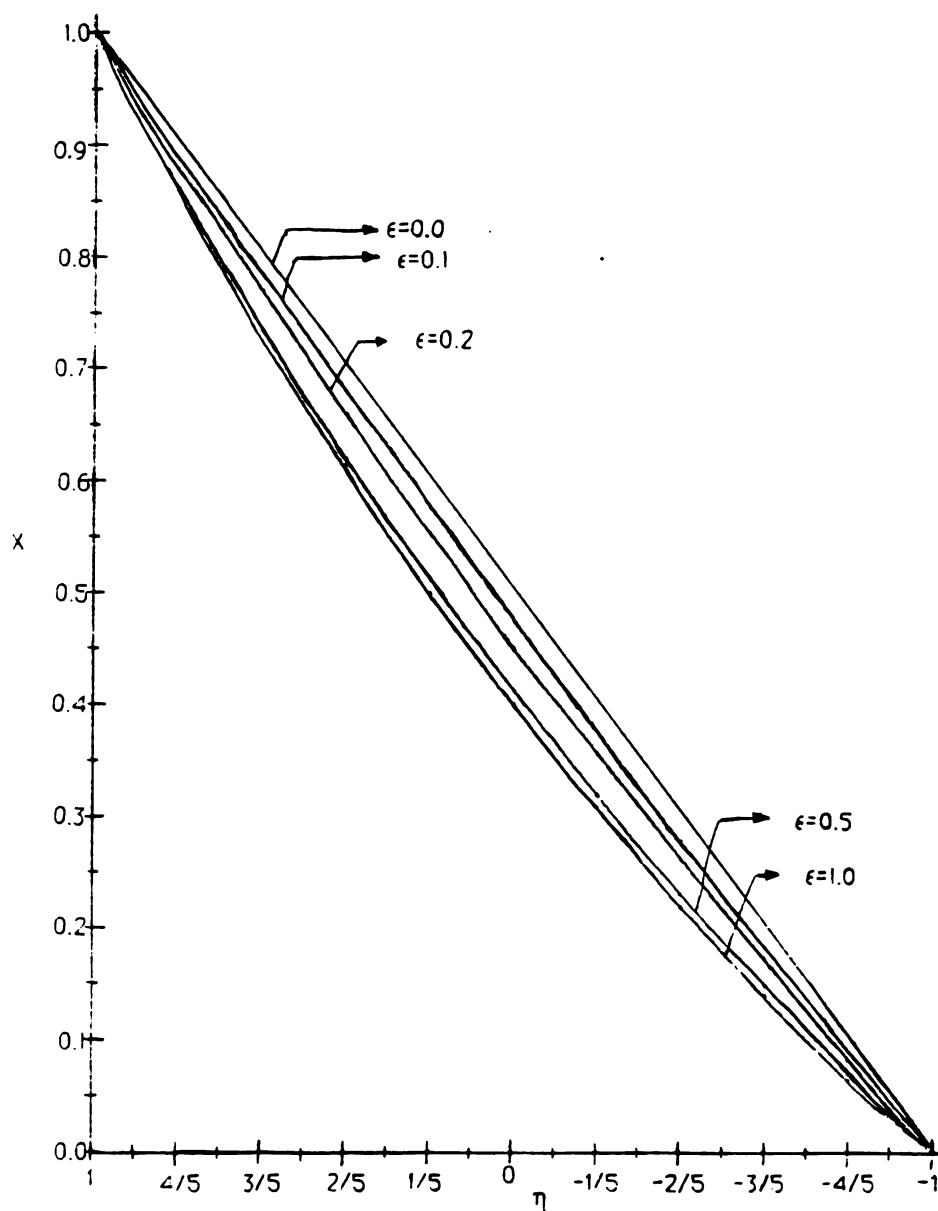


Figure 18.-- Dimensionless Temperatures along η -axis when $\theta = \pi/4$

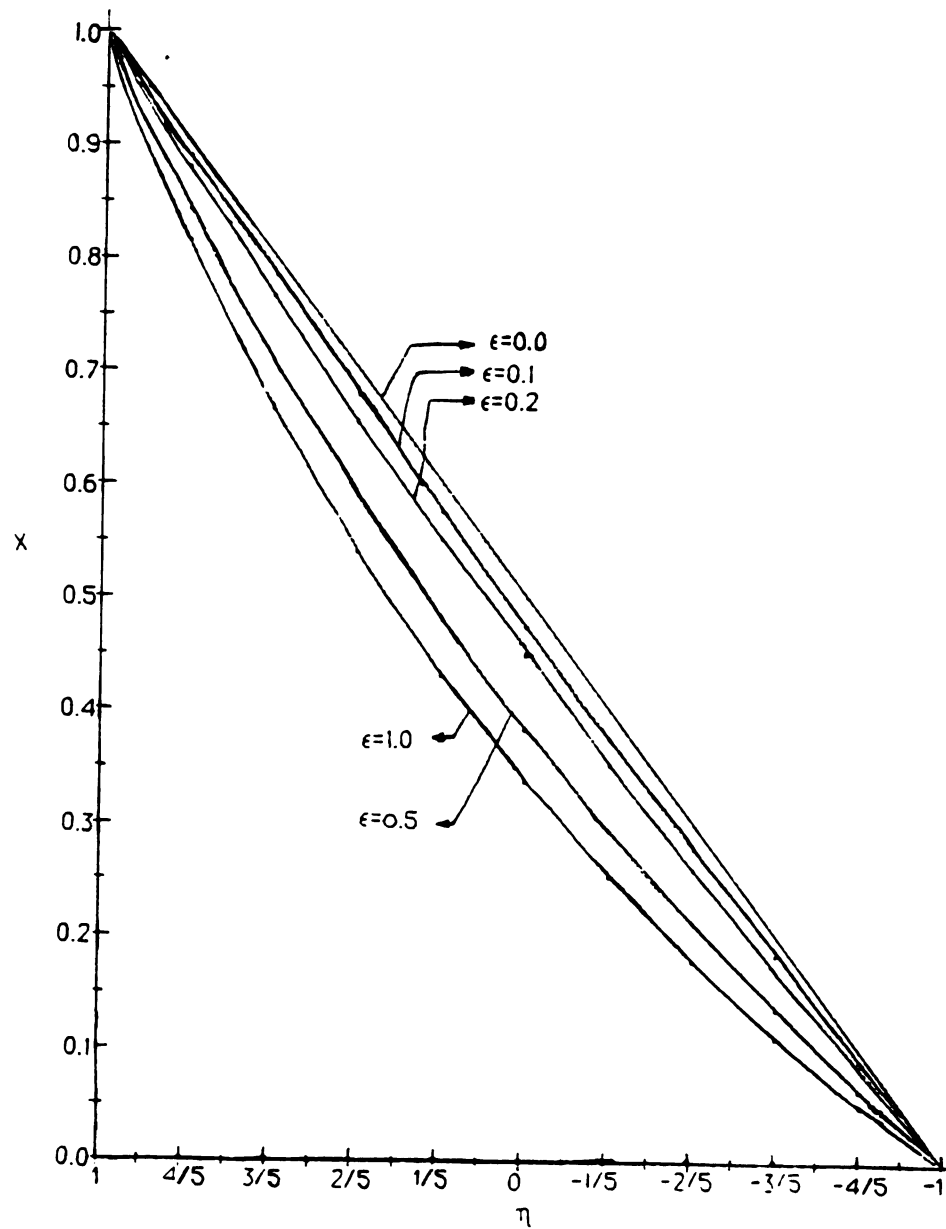


Figure 9.-- Dimensionless Temperatures along η -axis when $\theta = \pi/2$

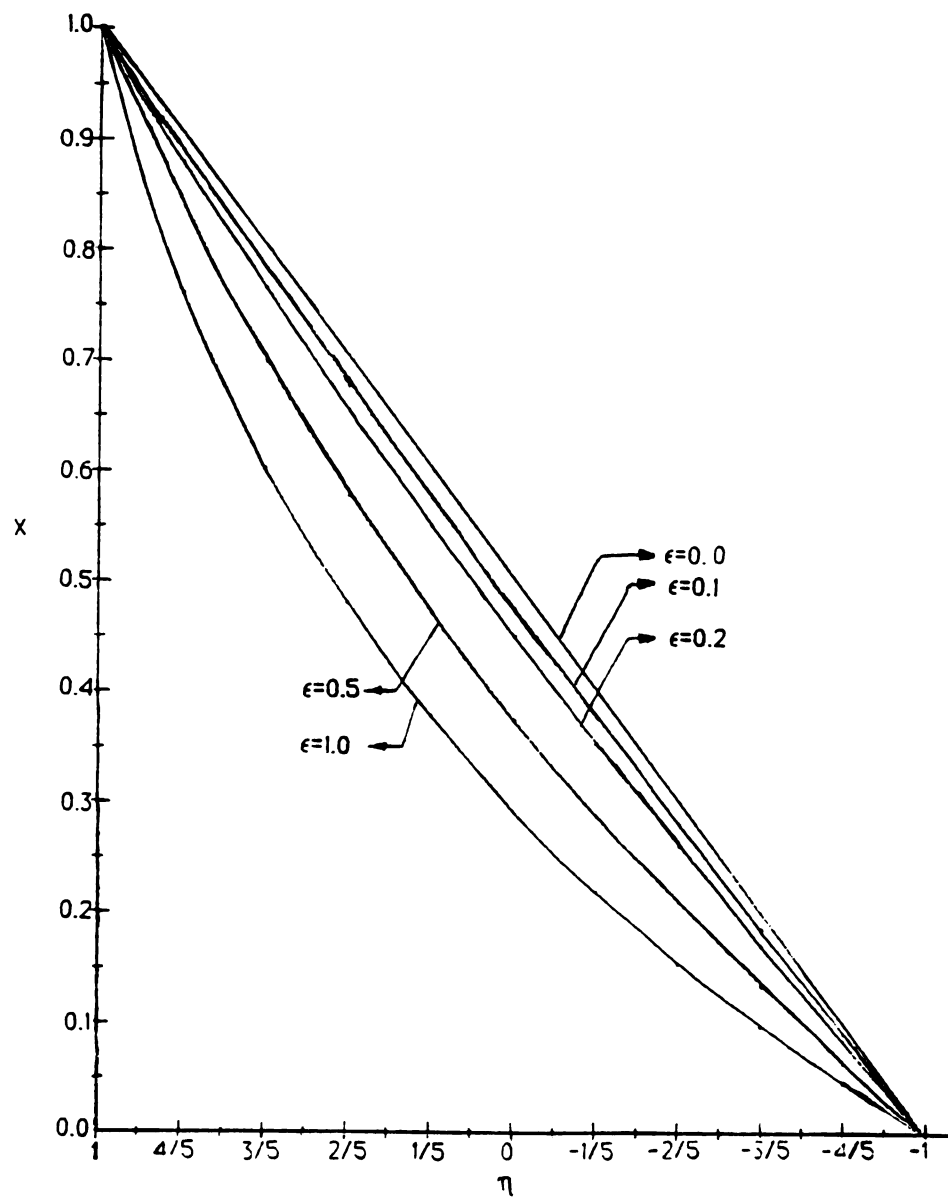


Figure 20.--Dimensionless Temperatures along η -axis when $\theta=3\pi/4$

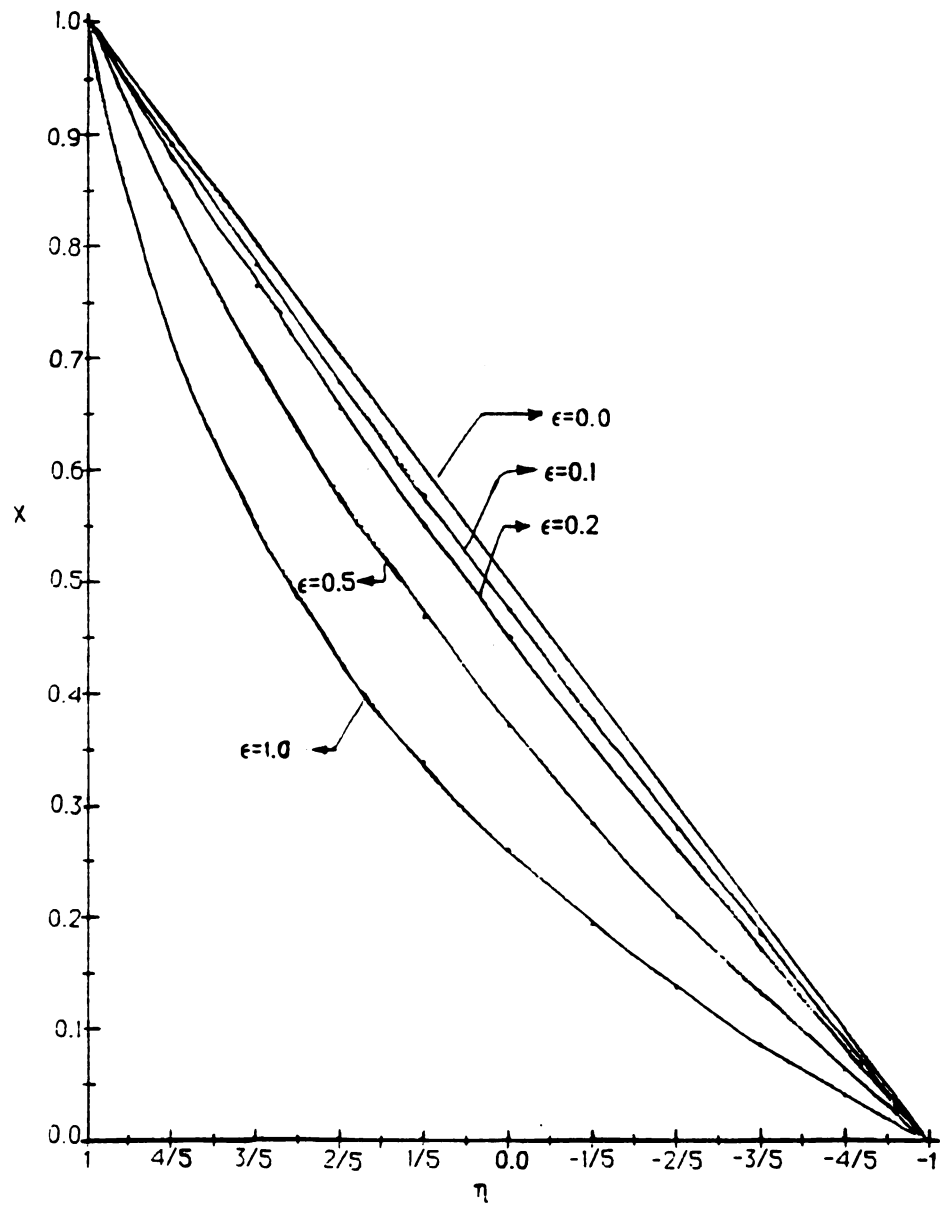


Figure 21.-- Dimensionless Temperatures along η -axis when $\theta = \pi$

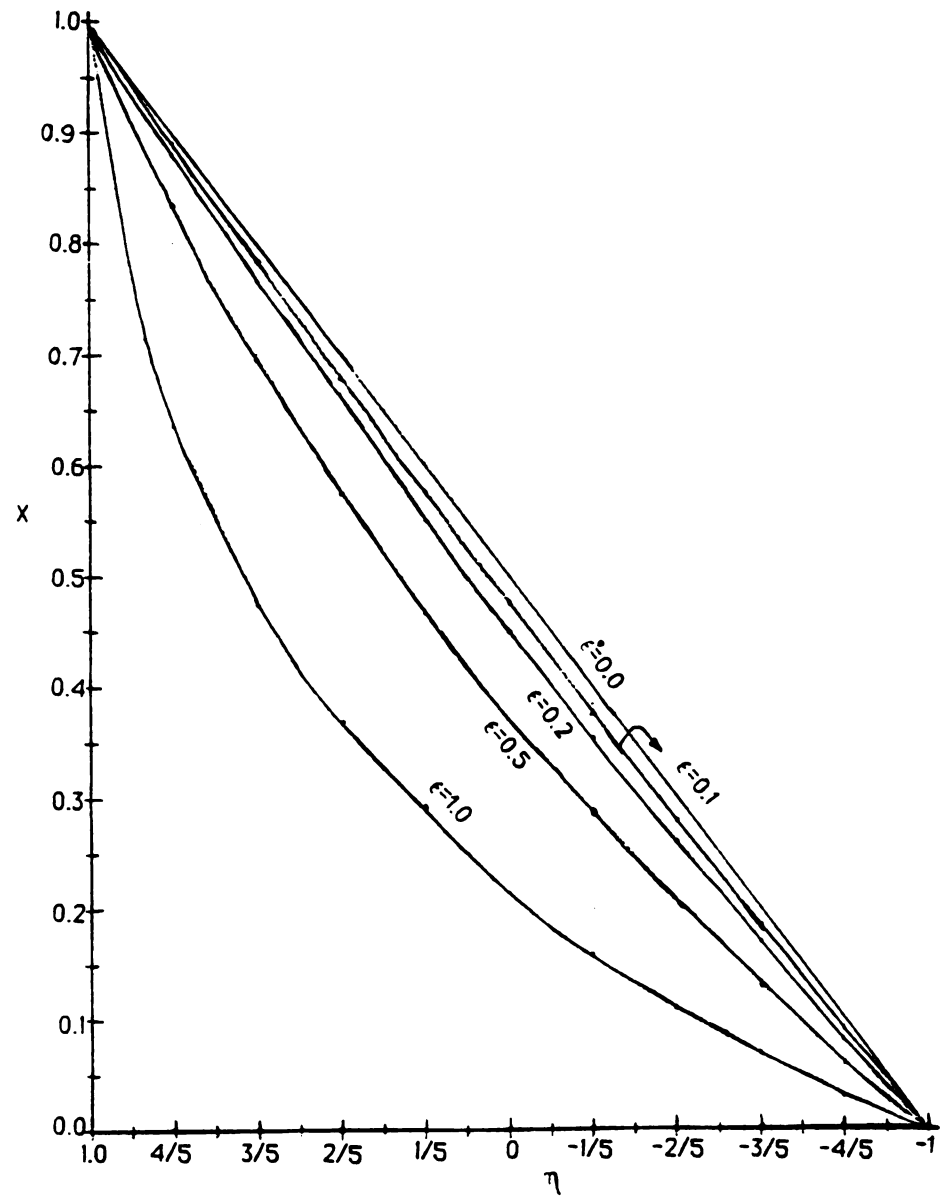


Figure 22.-- Dimensionless Temperatures along η -axis when $\theta = 3\pi/2$

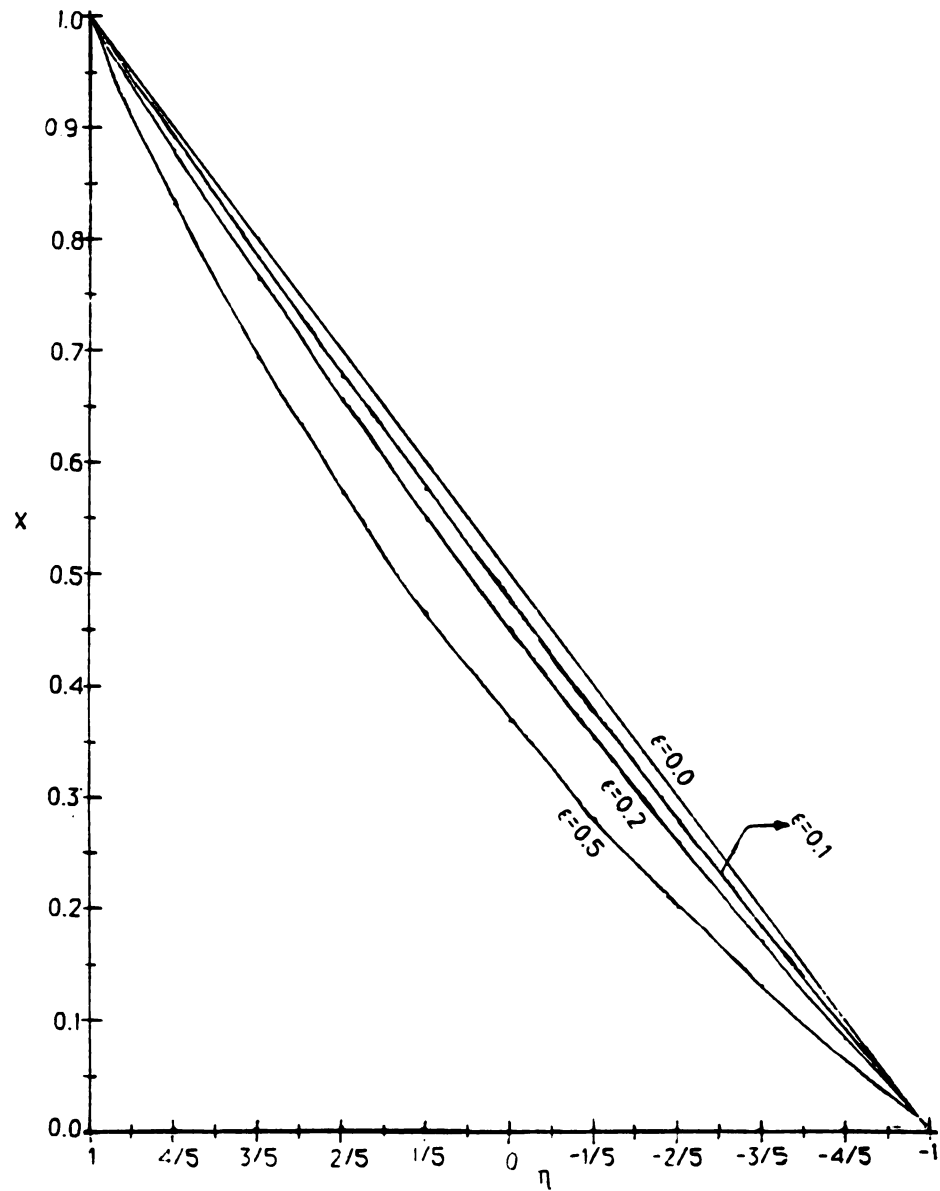


Figure 23.-- Dimensionless Temperatures along η -axis when $\theta=2\pi$

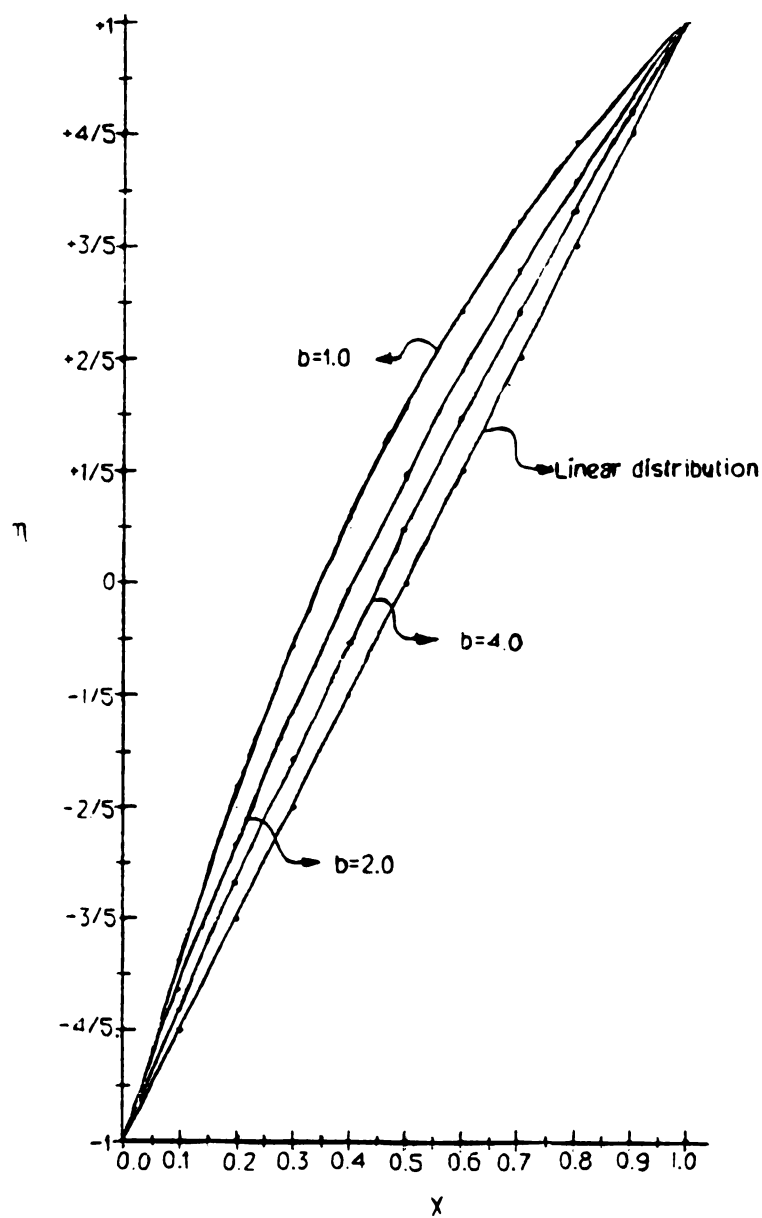


Figure 24.--Location of the intersection of the different isotherms with η -axis when $\theta = \pi/2$

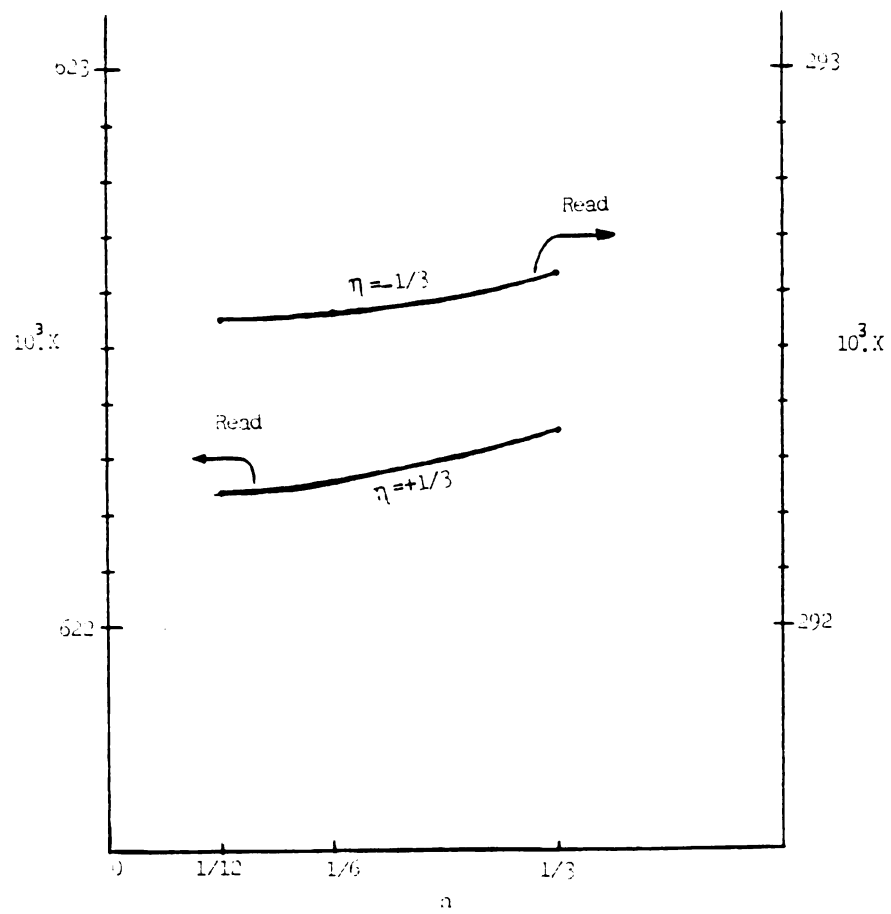


Figure 15.—The Dimensionless Temperatures verses h at Two Locations Along η -axis

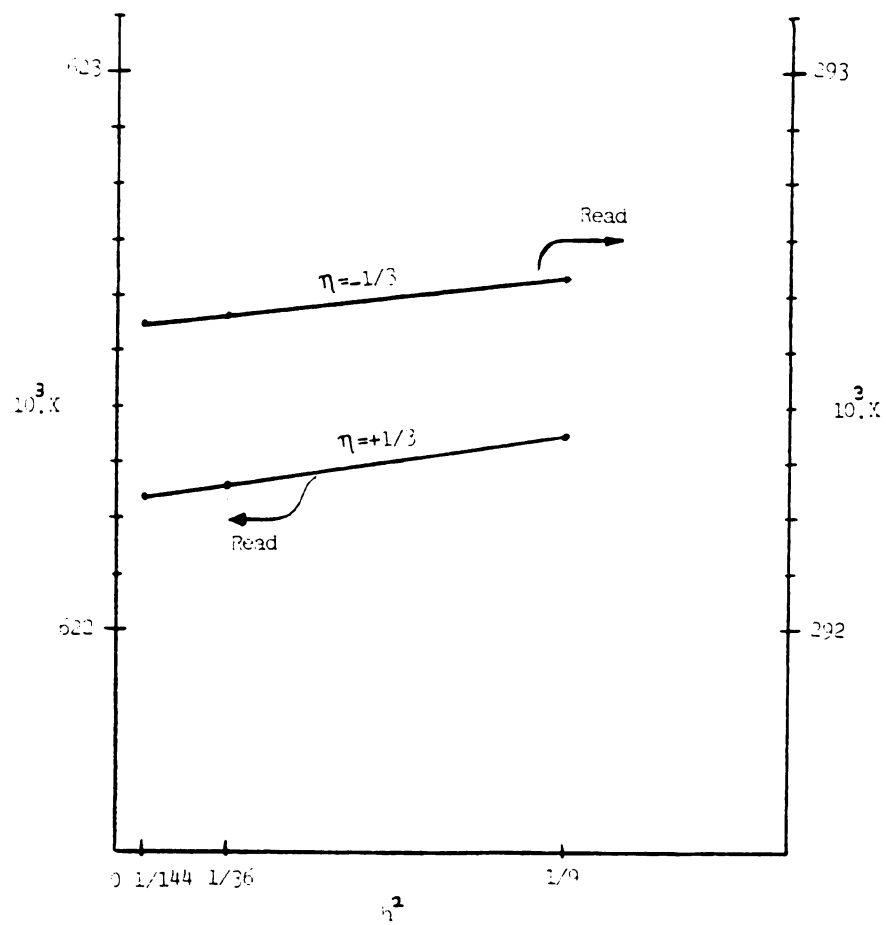


Figure 26.—The dimensionless Temperatures versus h^2 at Two Locations Along The η -axis

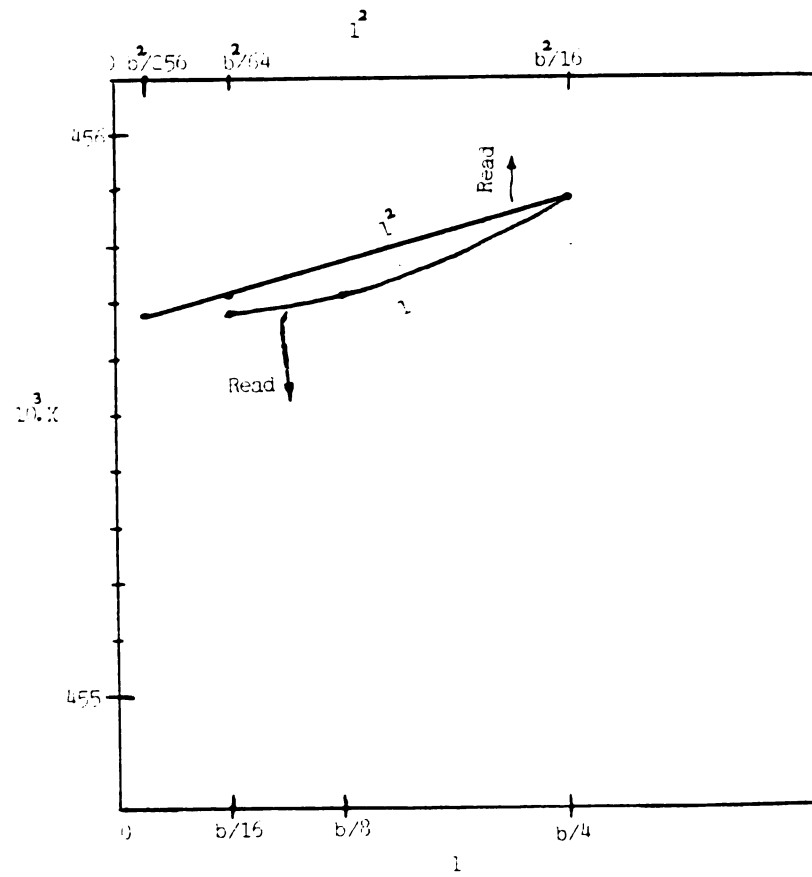


Figure 27.—The Dimensionless Temperatures at $c=b/2$ Along The c -axis versus l (bottom line) and l^2 (top line)

APPENDIX

APPENDIX

THE COMPUTER PROGRAM

```

1  PROGRAM ATHENA
    REAL A(198,198),B(198,1),E(9),G(9),U(5),WKAREA(198),
      Z(9)
    INTEGER L(11),M,N,MA,IB,IDGT,IER
    OPEN(20,FILE='OUTPUT')
5  C IN THIS PROGRAM, FIRST THE VALUES OF  $\epsilon$ , l, h, b AND  $\theta$  ARE
    C CALCULATED AND THEN THE SUBROUTINES SKY1 AND SKY2
    C ARE CALLED TO FORM THE ELEMENTS OF A AND B MATRICES.
    C THEN THE SUBROUTINE 'LEQTLF' IS CALLED TO SOLVE THE
10 C EQUATION AX=B.
    C VARIABLES: L(1) IS THE NUMBER OF DIVISIONS ALONG  $\eta$ -axis
    C L(2) IS THE NUMBER OF DIVISIONS ALONG s-axis IN THE
    C CURVED SEGMENT. L(3) IS THE NUMBER OF DIVISIONS ALONG
    C s-axis ONLY IN THE STRAIGHT SEGMENTS OF THE PLATE.
15 C C REPRESENTS l WHICH IS THE LENGTH OF MESH ALONG
    C s-axis. H REPRESENTS h WHICH IS THE LENGTH OF MESH
    C ALONG  $\eta$ -axis. W STANDS FOR  $\epsilon=a/R$ .
      L(1)=9
      L(2)=5
20  L(3)=15
      L(4)=L(1)*L(2)+L(1)
      L(5)=L(1)*L(2)+L(1)*L(3)+2*L(1)
      L(6)=L(1)+1
      L(8)=L(1)*L(2)+L(1)+1
25  L(9)=L(1)*L(2)+2*L(1)
      L(10)=L(5)-L(1)
      L(11)=L(2)+1
      U(1)=L(11)
    C HERE THE MESH LENGTHS ARE CALCULATED.
30  C C IS EQUAL TO SMALL l
      C=B/U(1)
      U(2)=L(6)
      H=2.0/U(2)
      W=0.5
35  C NOW THE ELEMENTS OF THE A MATRIX ARE BEING FORMED.
      R=(C**2)/(H**2)
      U(3)=- (2.0+2.0*R)
      D=((L(1)-1)/2)+1
      DO 2 I=1,L(1)

```

```

40      D=D-1.0
        E(I)=- (2.0+R*2.0* ((1.0-W*H*D)**2))
        F(I)=(R* ((1.0-W*H*D)**2)+W* (W*D*H-1.0)* (C**2)/(2.0*H))
        G(I)=R* ((1.0-W*H*D)**2)-W* (W*H*D-1.0)* ((C**2)/(2.0*H))
        Z(I)=E(1)-R*2.0-2.0
45      IF (I.EQ.1) THEN
        U(4)=F(I)
        U(5)=F(I)+R
        ELSE
        END IF
50      2 CONTINUE
C      HERE IT MAKES A CALL TO THE SUBROUTINE SKY1 WHICH FORMS
C      ELEMENTS OF MATRIX A
        CALL SKY1(A,L,E,G,F,Z,U)
        SUBROUTINE SKY1
55      REAL A(198,198),E(9),F(9),G(9),U(9),Z(9)
        INTEGER L(11)
        DO 3 I=1,L(11)
        DO 4 L=1,L(5)
        IF (I.EQ.J) THEN
60      A(I,J)=E(1)
        ELSE IF (I.EQ.L(1).AND.J.EQ.L(6)) THEN
        A(I,J)=0.0
        ELSE IF (J.EQ.I+1) THEN
        A(I,J)=G(i)
65      ELSE IF (J.EQ.L(1)+I) THEN
        A(I,J)=2.0
        ELSE IF (J.EQ.I-1) THEN
        A(I,J)=F(I)
        ELSE
70      A(I,J)=0.0
        END IF
        4 CONTINUE
        3 CONTINUE
        DO 8 I=L(6),L(4)
75      DO 9 J=1,L(5)
        K=I/L(1)
        M=1-K*L(1)
        L(7)=K*L(1)+1
        IF (I.EQ.J.AND.I.NE.K*L(1)) THEN
80      A(K,J)=E(M)
        ELSE IF (I.EQ.J.AND.I.EQ.K*L(1)) THEN
        N=L(1)
        A(I,J)=E(N)
        ELSE IF (I.EQ.L(7).AND.J.EQ.I-1) THEN
85      A(I,J)=0.0
        ELSE IF (I.EQ.K*L(1).AND.J.EQ.I+1) THEN
        A(I,J)=0.0
        ELSE IF (J.EQ.I-1.AND.I.NE.K*L(1)) THEN
        A(I,J)=F(M)
90      ELSE IF (J.EQ.I-1.AND.I.EQ.K*L(1)) THEN
        N=L(1)
        A(I,J)=E(N)

```

```

      ELSE IF (I.EQ.L(7).AND.J.EQ.I-1) THEN
      A(I,J)=0.0
100  ELSE IF (I.EQ.K*L(1).AND.J.EQ.I+1) THEN
      A(I,J)=0.0
      ELSE IF (J.EQ.I-1.AND.I.NE.K*L(1)) THEN
      A(I,J)=F(M)
      ELSE IF (J.EQ.I-1.AND.I.EQ.K*L(1)) THEN
105  N=L(1)
      A(I,J)=F(N)
      ELSE IF (J.EQ.I+1) THEN
      A(I,J)=G(M)
      ELSE IF (J.EQ.I-L(1)) THEN
110  A(I,J)=1.0
      ELSE IF (J.EQ.I+L(1)) THEN
      A(I,J)=1.0
      ELSE
      A(I,J)=0.0
115  END IF
      9 CONTINUE
      8 CONTINUE
      DO 12 I=L(8),L(9)
      DO 13 J=1,L(5)
120  K=I-L(4)
      IF (I.EQ.J) THEN
      A(I,J)=Z(K)
      ELSE IF (I.EQ.L(8).AND.J.EQ.I-1) THEN
      A(I,J)=0.0
125  ELSE IF (I.EQ.L(9).AND.J.EQ.I+1) THEN
      A(I,J)=0.0
      ELSE IF (J.EQ.I+1) THEN
      A(I,J)=G(K)+R
      ELSE IF (J.EQ.I-1) THEN
130  A(I,J)=F(K)+R
      ELSE IF (J.EQ.I-L(1)) THEN
      A(I,J)=2.0
      ELSE IF (J.EQ.I+L(1)) THEN
      A(I,J)=2.0
135  ELSE
      A(I,J)=0.0
      END IF
      13 CONTINUE
      12 CONTINUE
140  DO 17 I=L(9(+1),L(5)
      DO 16 J=1,L(5)
      K=I/L(1)
      N=L(1)
      IF (I.EQ.J) THEN
145  A(I,J)=U(3)
      ELSE IF (I.EQ.N*K.AND.J.EQ.I+1) THEN
      A(I,J)=0.0
      ELSE IF (I.EQ.N*K+1.AND.J.EQ.I-1) THEN
      A(I,J)=0.0
150  ELSE IF (J.EQ.I+1) THEN

```

```

      A(I,J)=R
      ELSE IF(J.EQ.I-1) THEN
      A(I,J)=R
      ELSE IF(I.LT.L(10)+1.AND.J.EQ.I+L(1)) THEN
155    A(I,J)=1.0
      ELSE
      A(I,J)=0.0
      END IF
160 16 CONTINUE
17 CONTINUE
      C HERE IT MAKES A CALL TO THE SUBROUTINE SKY2 WHICH FORMS
      C THE ELEMENTS OF MATRIX B
      CALL SKY2
165  SUBROUTINE SKY2
      REAL B(198,1),U(5)
      INTEGER L(11)
      DO 25 I=1,L(11)
      IF(I.EQ.J) THEN
170    DO 25 I=1,L(1)
      IF(I.EQ.1) THEN
      B(I,1)=U(4)
      ELSE
      B(I,1)=0.0
175    END IF
      25 CONTINUE
      DO 26 I=L(6),L(4)
      M=I/L(1)
      IF(I.EQ.M*L(1)+1) THEN
180    B(I,1)=-U(4)
      ELSE
      B(I,1)=0.0
      END IF
      27 CONTINUE
185    DO 28 I=L(9)+1,L(10)
      M=I/L(1)
      IF(I.EQ.M*L(1)+1) THEN
      B(I,1)=-R
      ELSE
190    B(I,1)=0.0
      END IF
      28 CONTINUE
      D=L(6)
      DO 29 I=L(10)+1,L(5)
195    D=D-1.0
      T=D/U(2)
      IF(I.EQ.L(10)+1) THEN
      B(I,1)=- (R+T)
      ELSE
200    B(I,1)=-T
      END IF
      29 CONTINUE
      C HERE THE DATA NEEDED FOR THE CALL FROM "IMSL" ARE SET UP
      N=L(5)

```



```
205     IDGT=3
        IB=L(5)
        IA=L(5)
        M=1
      C HERE THE CALL IS MADE TO THE ROUTINE "LEQT1F".
210     CALL LEQT1F(A,M,N,EA,B,IDGT,WKAREA,IER)
      C NOW THE OUTPUT IS CALLED TO PRINT THE RESULT OF
      C SOLUTION.
        DO 31 J=1,L(5)
        WRITE(20,30)B(J,1)
215 30  FORMAT(60X,F8.7)
        31 CONTINUE
        STOP
218     END
```

LIST OF REFERENCES

LIST OF REFERENCES

1. Carslaw, H.S. and Jaeger, J.C., Conduction of Heat in Solids, University Press, Oxford, 2nd Edition, 1959, pp. 445-446.
2. Ozisik, M.N., Heat Conduction, Wiley, New York, 1980, pp. 471-516.
3. Carslaw, H.S., Introduction to the Mathematical Theory of the Conduction of Heat in Solids, Dover, New York, 1945.
4. Wang, C.Y., "A New Analytical Method for the Heat Conduction Across a Bent Plate," Letters in Heat and Mass Transfer, Vol. 9, 1982, pp. 199-207.
5. Wang, C.Y., "Flow in Narrow Curved Channels," Journal of Applied Mechanics, Vol. 47, 1980, pp. 7-10.
6. Holman, J.R., Heat Transfer, McGraw Hill, 4th Edition, 1976, pp. 63-86.
7. Ozisik, M.N., Boundary Value Problems of Heat Conduction, International Text Book, Pa., 1968.
8. Sokolnikoff, I.S., Tensor Analysis--Theory and Applications to Geometry and Mechanics of Continua, Chapter 3, Wiley, New York, 1964.